



1 **Characterization of dissolved organic matter in surface water and** 2 **groundwater: a dataset for the Seine River basin (France)**

3 Fulvia Baratelli¹, Edith Parlanti², Josette Garnier¹, Gilles Varrault³, Angélique Goffin³, Nadège
4 Musabimana³, Sabrina Guérin Rechdaoui⁴, Vincent Rocher⁴, Nicolas Flipo⁵

5 ¹Sorbonne Université, CNRS, EPHE, UMR Metis 7619, F-75005 Paris, France

6 ²Univ. Bordeaux, CNRS, Bordeaux INP, EPOC, UMR 5805, F-33600 Pessac, France

7 ³LEESU, Univ. Paris Est Creteil, ENPC, Institut Polytechnique de Paris, Creteil, France

8 ⁴SIAAP, Direction Innovation, Colombes, France

9 ⁵Mines ParisTech, PSL University, Centre for Geosciences and Geoengineering, 77300 Fontainebleau, France

10

11 *Correspondence to:* Fulvia Baratelli (fulvia.baratelli@minesparis.psl.eu)

12 **Abstract.** Carbon fluxes in river networks represent a major component of the carbon cycle, but they are
13 difficult to estimate at large scale. In particular, the physicochemical properties of organic matter (OM)
14 and its contribution to river carbon fluxes remain poorly understood. In this context, this paper presents a
15 dataset for quantifying and characterizing dissolved organic carbon (DOC) in a regional river basin, the
16 Seine River basin in France (76 000 km²), which is subject to numerous human pressures. The dataset is
17 the result of several sampling campaigns conducted over a 14-year period (2011–2024). A total of 1047
18 samples were collected from various water types (surface water, groundwater and treated effluents from
19 wastewater treatment plants, WWTPs) at sites across the basin encompassing diverse land uses. Dissolved
20 organic matter (DOM) was characterized both quantitatively, by measuring the concentration of dissolved
21 organic carbon (DOC), and qualitatively, through analysis of its optical properties using UV-Visible
22 absorbance and excitation–emission matrix (EEM) fluorescence spectroscopy. Additionally, using the 45-
23 day incubation method, the biodegradable fraction of DOC, which plays a particularly significant role in
24 river water quality, was estimated for 27 % of the samples. The content and properties of OM in the Seine
25 River basin vary significantly depending on the site, measurement period, and type of water sampled.
26 DOC concentrations are generally higher in WWTP discharges and gravel pits. The biodegradable
27 fraction of DOC is higher in samples from WWTP discharges and from groundwater in a forested alluvial
28 plain. OM in the basin generally displays a low level of aromaticity but is hydrophilic and characterized
29 by strong biological activity. This biological activity is particularly pronounced in the treated effluents



30 from small-capacity WWTPs, where OM is mainly of microbial origin, and in gravel pits, where OM
31 consists primarily of protein-type compounds. Groundwater typically contains a mixture of OM of both
32 terrestrial and microbial/biological origins. These data may be useful for future studies of (i) the organic
33 carbon cycle at the regional basin scale, (ii) the characteristics of OM across different compartments of a
34 hydrosystem, and (iii) river metabolism. The dataset is available at
35 <https://data.indores.fr/privateurl.xhtml?token=a6b58980-3280-4a1b-9311-a0b401955e75>.

36 **1 Introduction**

37 Land-to-ocean transport of carbon through the land-to-ocean aquatic continuum (LOAC; Regnier et al.,
38 2022) is increasingly recognized as a major component of the carbon cycle at both regional and global
39 scales (Battin et al., 2023, 2009). These transfers of carbon occur by means of physical, chemical, and
40 biological processes both within the LOAC, which includes inland waters, estuaries, tidal wetlands, and
41 continental shelf waters, and between the LOAC and the other Earth compartments (atmosphere,
42 biosphere, lithosphere).

43 These aquatic carbon fluxes are difficult to quantify at large scale and they are often overlooked or only
44 partially considered in global carbon budget assessments and land-surface models. The global carbon
45 budget (Friedlingstein et al., 2023) does not include the metabolism of surface waters (rivers, lakes, and
46 reservoirs) and estuarine waters, which contribute an additional 0.75 GtC yr^{-1} to the atmosphere (Cole et
47 al., 2007). Regarding terrestrial carbon, land-surface models that omit land-to-ocean lateral carbon
48 transfer may lead to an overestimation of 4.5 % in the simulated annual net terrestrial carbon uptake across
49 Europe (Zhang et al., 2022). Further, according to Regnier et al. (2022), ignoring the LOAC carbon fluxes
50 results in an overestimation of carbon storage in terrestrial ecosystems by $0.6 \pm 0.4 \text{ Pg}$ of carbon per year
51 and an underestimation of sedimentary and oceanic carbon storage. More data are needed to reduce
52 uncertainties in estimating lateral inorganic and organic carbon fluxes and their spatiotemporal variations
53 (Yan et al., 2023; Zhang et al., 2022).



54 It is thus crucial to improve our understanding of the mechanisms associated with the carbon fluxes in the
55 LOAC and to take them into account when evaluating the global carbon balance and its response to
56 climatic and anthropogenic stresses.

57 Within the LOAC, river networks in particular can be considered biogeochemical reactors (Battin et al.,
58 2023), where several processes and reactions control carbon fluxes. Carbon in riverine environments is
59 present in different forms: greenhouse gases (CO₂ and CH₄); inorganic carbon from soils and from rock
60 alterations; and organic carbon from organic matter (OM), mainly from terrestrial, riparian, or aquatic
61 vegetation. According to estimates that take into account only permanent waters and in some cases also
62 peripheral flood zones, between 2 and 5 Pg of carbon transits annually through the world's rivers (Battin
63 et al., 2023; Cole et al., 2007; Drake et al., 2018; Raymond et al., 2013). The “active pipe concept” (Cole
64 et al., 2007) shows that only 0.9 Pg of this carbon reaches the ocean, because the continental hydrosphere
65 has three key roles of (i) emitting CO₂ and CH₄ to the atmosphere, (ii) storing organic carbon in river
66 sediments and floodplains, and (iii) exporting to the ocean both bicarbonates produced by rock alterations
67 and slowly biodegradable organic carbon.

68 Despite its key role in environmental processes, the contribution of OM to river carbon fluxes remains
69 poorly understood. OM is a highly complex and dynamic mixture of organic compounds from both natural
70 and anthropogenic sources (Artifon et al., 2019; Cawley et al., 2012; Bauer et al., 2011). The
71 allochthonous (detritus from terrestrial plants and soils) or autochthonous (*in situ* aquatic production)
72 origin of natural OM in rivers and aquatic ecosystems determines its composition and physicochemical
73 properties, which influence its (photo-)chemical and biological transformation, its reactivity, and its role
74 in the carbon cycle (Besemer et al., 2009; Lambert et al., 2017; Carlson and Hansell, 2015). The
75 concentration and composition of OM also depend on the properties of the surrounding watershed and on
76 the hydrological connectivity between rivers, oxbows, and groundwater, which control the transfer of
77 terrestrial and aquatic OM in riverine ecosystems. Organic carbon is mostly described as dissolved
78 organic carbon (DOC), which is more abundant than particulate organic carbon (Alvarez-Cobelas et al.,
79 2012). Terrestrial organic carbon has long been considered recalcitrant and conservatively transported
80 along river networks, with minimal contribution to aquatic metabolism. Contrary to previous
81 assumptions, several studies carried out over the past two decades have shown that it is much less



82 refractory and hence more bioavailable than previously thought (Besemer et al., 2009; Battin et al., 2008;
83 Wiegner et al., 2009). Human activities also modify the properties of fluvial OM, with inputs from
84 agricultural and forestry practices as well as from urban, domestic, and industrial discharges (Artifon et
85 al., 2019; Cawley et al., 2012). Biodegradable OM plays a particularly significant role in river water
86 quality. Large inputs of biodegradable OM can disrupt the dissolved oxygen cycle, leading to transient or
87 permanent water anoxia (Tusseau-Vuillemin and Le Reveillé, 2001).

88 Not only the quantity but also the quality of organic carbon reflects the dynamic interactions between OM
89 sources and biogeochemical processes (Jaffé et al., 2008), and both are likely to have ecological
90 repercussions (Cory et al., 2011; Jaffé et al., 2014). The chemical composition of organic carbon is
91 modified by biogeochemical processes, including bacterial activity. These changes in the composition of
92 organic carbon, in turn, influence heterotrophic activity, CO₂ release, the biogeochemistry of nutrients
93 and pollutants, and the formation of disinfection by-products in drinking water treatment plants (Zhuang
94 and Yang, 2018).

95 It is thus essential to improve our knowledge of the physicochemical properties of OM and our ability to
96 characterize its composition and reactivity.

97 In this context, we present a comprehensive dataset to quantify and characterize dissolved organic matter
98 (DOM) in a regional river basin such as the Seine River basin in France, which is subject to numerous
99 human pressures that influence the carbon structure in the various compartments of the hydrosystem. This
100 dataset is the result of several sampling campaigns carried out over a 14-year period (2011–2024) in the
101 framework of the PIREN-Seine research program (<https://www.piren-seine.fr/en>). The water samples
102 were collected at sites representative of different land uses in the Seine River basin (agricultural and
103 urban) and in different compartments of the hydrosystem: surface water, groundwater, and treated
104 effluents from wastewater treatment plants (WWTPs). The dataset includes variables that characterize
105 DOM both quantitatively and qualitatively using a combination of approaches and methods.

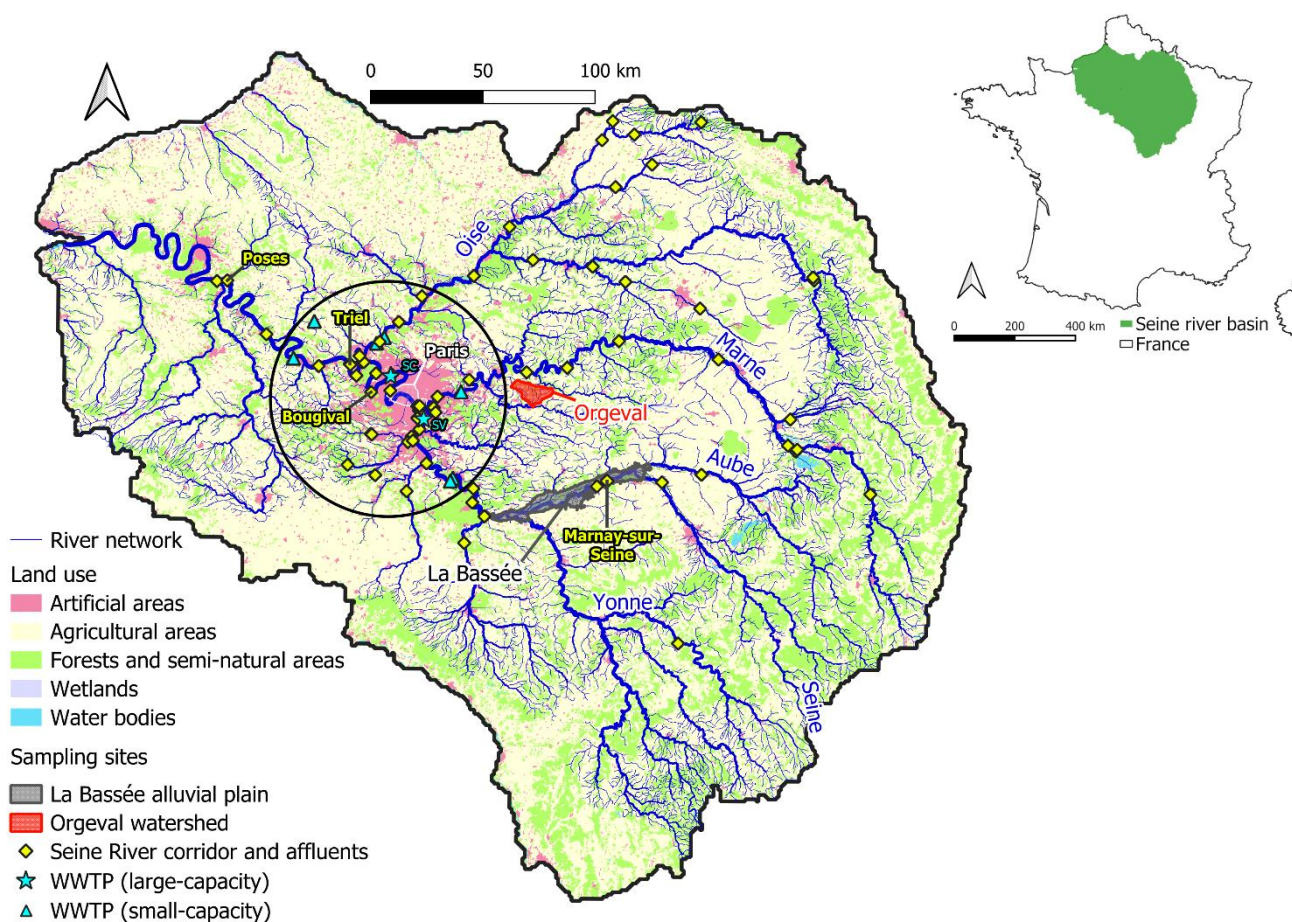
106 The dataset will remain accessible to the scientific community in order to pose new research questions
107 related to: river metabolism; the sources, dynamics, and transformations of OM in surface water, in
108 groundwater, and at their interface; and the typology of organic carbon in a basin at the regional scale.



109 These observational data could also be used to parameterize and evaluate land-surface models or models
110 assessing the quality of river networks.

111 2 Study area

112 The Seine River basin (76 000 km²), located in northern France (Fig. 1), is the most urbanized and
113 industrialized basin in France (Billen et al., 2007; Flipo et al., 2021). Given its large population and
114 intensive cereal production, the water resources of the Seine River basin are of high strategic importance.
115 As a major urban center, Paris relies heavily on the Seine River to meet its water needs. However, the
116 city's dense population and industrial activities contribute significantly to the pollution of the river, posing
117 challenges for water quality and ecosystem health.



118



119 **Figure 1: Seine River basin and sampling sites considered in this study: La Bassée alluvial plain (gray, see Fig. 2); the Orgeval**
120 **watershed (red, see Fig. 3); the Seine River corridor and its tributaries (yellow diamonds); the small-capacity WWTPs (blue**
121 **triangles); the two large-capacity WWTPs (blue stars: SA is Seine Aval and SV is Seine Valenton). The area in the black circle is**
122 **zoomed in Fig. 4. The hydrographic network is represented with a line of increasing thickness according to Strahler's order. Source**
123 **of land use map: Corine Land Cover 2018, European Union's Copernicus Land Monitoring Service information.**

124
125 The climatic regime of the Seine River basin is pluvial/oceanic, modulated by seasonal variations in
126 evapotranspiration. The average precipitation ranges from 1200 mm yr⁻¹ along the coastal shoreline and
127 in the upstream mountainous area to 650 mm yr⁻¹ in the central part of the basin, whereas the average
128 precipitation for the entire basin is 800 mm yr⁻¹. The total river network comprises 27 500 km of streams,
129 and the main course of the Seine River is 777 km long (Marescaux et al., 2020). The hydrological regime
130 is pluvial/oceanic, with a high-flow period in winter and a low-flow period in summer. The mean annual
131 discharge at the Poses gauging station, which is located in the most downstream part of the river network
132 at the entrance of the estuary (Fig. 1), is 509 m³ s⁻¹ (average during the period 1990–2006). The
133 hydrological regime is very irregular due to intense floods and droughts. For example, the mean daily
134 discharge at Poses is 179 m³ s⁻¹ during 5-year droughts and 2 590 m³ s⁻¹ during 20-year floods. Land use
135 in the Seine River basin (Fig. 1) is mainly represented by croplands (56.5 %), followed by forested areas
136 (25.6 %), grasslands (9.5 %), and urbanized areas (7.6 %).

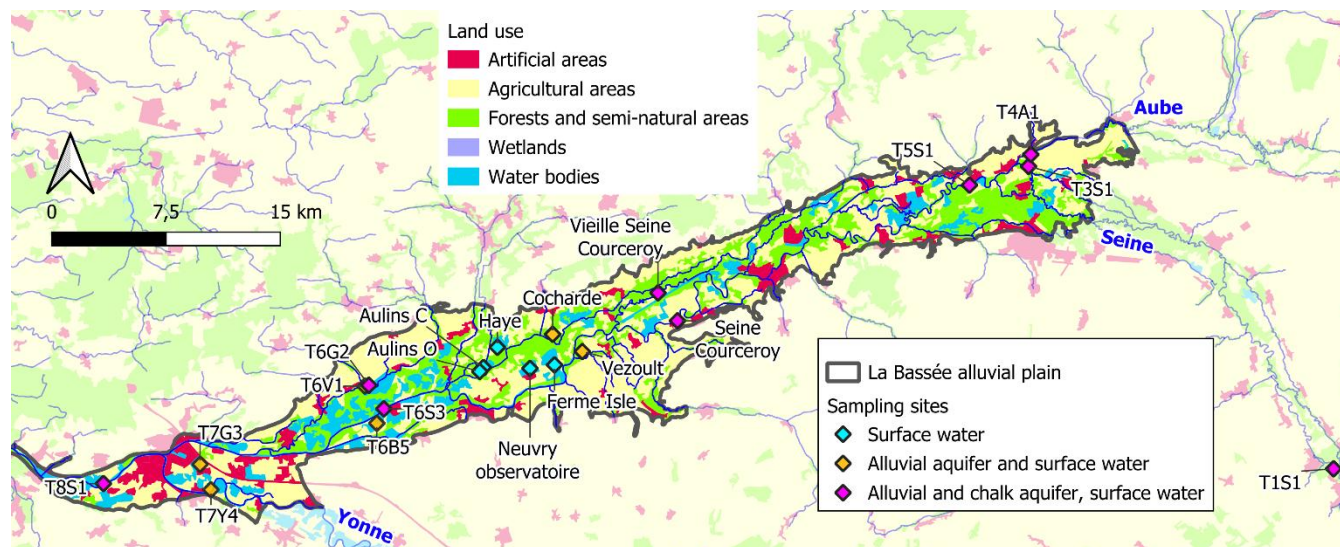
137 The data presented in this paper were obtained from water samples collected at several sites in the Seine
138 River basin, representative of various land uses (Fig. 1): an alluvial plain (La Bassée), a small rural and
139 agricultural watershed (Orgeval), several sites along the Seine River and some of its main tributaries
140 (Marne River, Oise River, Aube River, Yonne River), as well as some minor tributaries. Treated effluents
141 from a number of WWTPs were also sampled (Fig. 1). All these samples are representative of different
142 compartments of the Seine hydrosystem: groundwater from aquifers of various depths (alluvial aquifer,
143 riverbank aquifer, Tertiary Brie aquifer, Upper Cretaceous chalk aquifer), surface water (rivers, gravel
144 pits, springs, oxbow lakes, ponds, agricultural drains), and treated effluents from WWTPs of various
145 capacities.



146 **2.1 La Bassée alluvial plain**

147 La Bassée is a part of the alluvial plain of the Seine River. It is located upstream of Paris, between the
148 confluences of the Seine River with two tributaries: the Aube River and the Yonne River. The alluvial
149 plain is 60 km long and 8 km wide and its surface area is around 320 km² (Flipo et al., 2021). The substrate
150 of the alluvial plain is mainly Upper Cretaceous chalk. La Bassée is a territory of major political,
151 economic, and environmental importance. It is a wetland of national importance for its remarkable
152 biodiversity, and it represents an important source of drinking water for the Paris region. Several
153 economic interests coexist here, including a nuclear power plant, a navigation channel, and numerous
154 gravel extraction sites, as well as development projects such as the construction of flood control
155 reservoirs. For these reasons, La Bassée has been studied by the PIREN-Seine research program for some
156 30 years. Numerous studies have been carried out in a wide range of disciplines, including geology,
157 hydro(geo)logy, geography, geochemistry, and geohistory (Lestel et al., 2018; Flipo et al., 2021).

158 A network of LOcal MONitoring Stations (LOMOS, Mouhri et al., 2013) was created in 2015, with the
159 objective of studying the interactions between surface water and groundwater. These stations consist of
160 one or two piezometers and a surface water device, all equipped with sensors to continuously measure
161 pressure and temperature in surface water (river, gravel pit, or oxbow lake), in the associated alluvial
162 aquifer, and, at some sites, also in the underlying chalk aquifer. Surface water and groundwater samples
163 were collected at each LOMOS station. Other surface water bodies were also sampled to enrich the dataset
164 with samples from gravel pits and oxbow lakes. All the sampling points in La Bassée are shown in Fig. 2.



165
166
167
168
169

Figure 2: Sites sampled in La Bassée alluvial plain. Source of land use map: Corine Land Cover 2018, European Union's Copernicus Land Monitoring Service information.

170 2.2 The Orgeval watershed

171 The 104 km² Orgeval watershed is located 70 km east of Paris (Garnier et al., 2014; Mouhri et al., 2013).
172 It is a sub-catchment of the Marne River basin, which is part of the Seine River basin (Fig. 1). The Orgeval
173 watershed aquifer system is composed of two main geological units: the Brie limestone Oligocene aquifer
174 and the deeper Champigny limestone Eocene aquifer. These two aquifer units are separated by a clayey
175 aquitard (green clays and marls) and are covered by a loess layer approx. 2–10 m thick. Land use is mostly
176 agricultural (82 %), dominated by cereal crops (wheat, maize, barley). The remaining surface is covered
177 by woods (17 %) and urban zones or roads (1 % of the surface). The Orgeval watershed is representative
178 of the headwaters of the Seine hydrosystem, characterized by extensive agricultural coverage. It is also
179 representative of a multi-layer aquifer system that exchanges water and nutrients with a river network
180 under temperate climate conditions.

181 The Orgeval watershed is a critical zone observatory and is part of the French Research Infrastructure
182 OZCAR (Floury et al., 2019; Gaillardet et al., 2018). It has been a long-term experimental observatory
183 and research site for 60 years (<https://gisoracle.inrae.fr/>). This site has been equipped with monitoring



184 stations for decades, enabling the measurement of a large number of physicochemical variables. In
185 particular, some LOMOS stations were installed to measure pressure and temperature in the river and in
186 the underlying aquifers, with the aim of understanding the interactions between groundwater and surface
187 water. Surface water and groundwater sampling points (Fig. 3) are representative of different types of
188 water and positions in the watershed. Surface water types include rivers, springs, agricultural drains, and
189 ponds. Groundwater types include colluvium and the Brie limestone Oligocene aquifer.

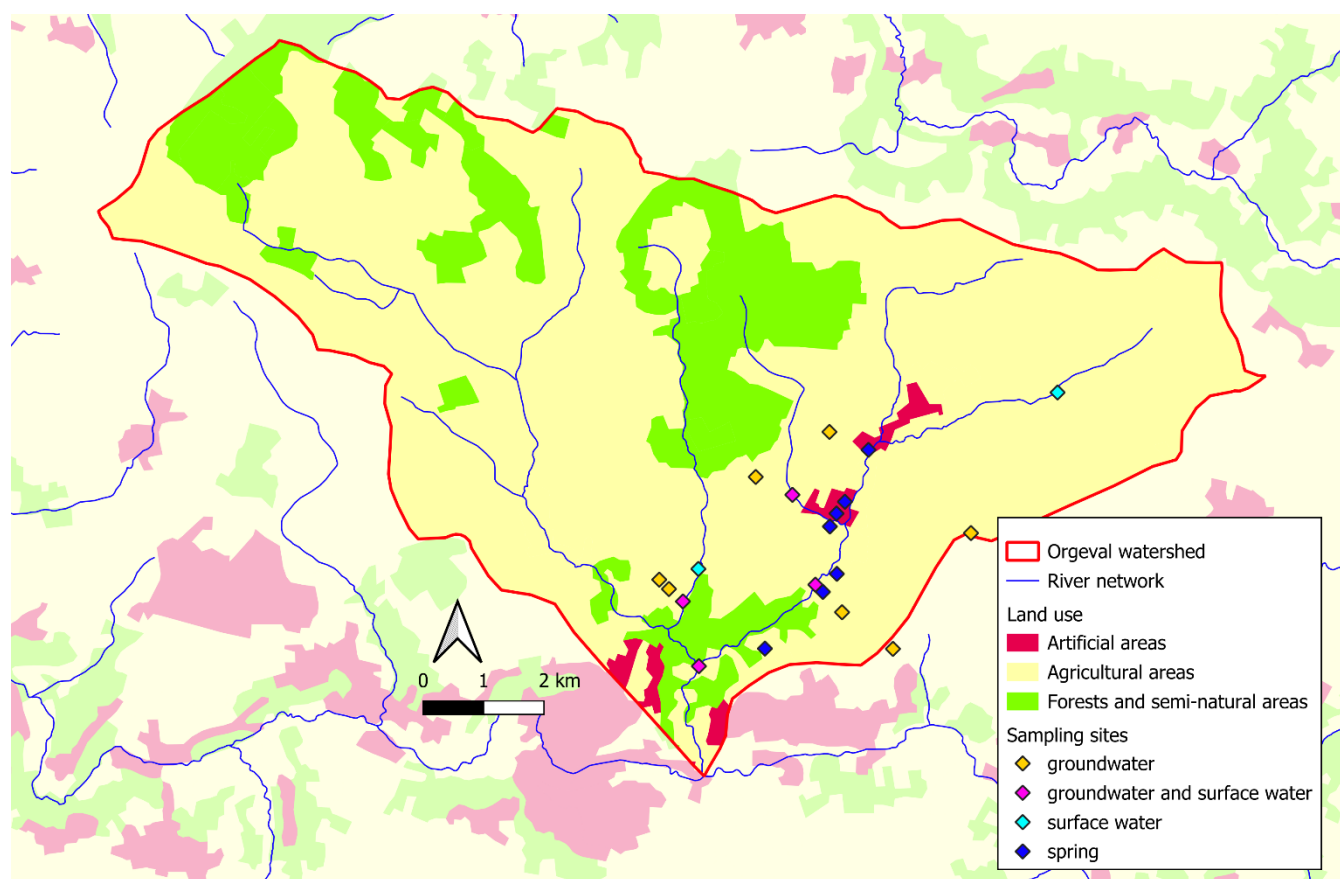


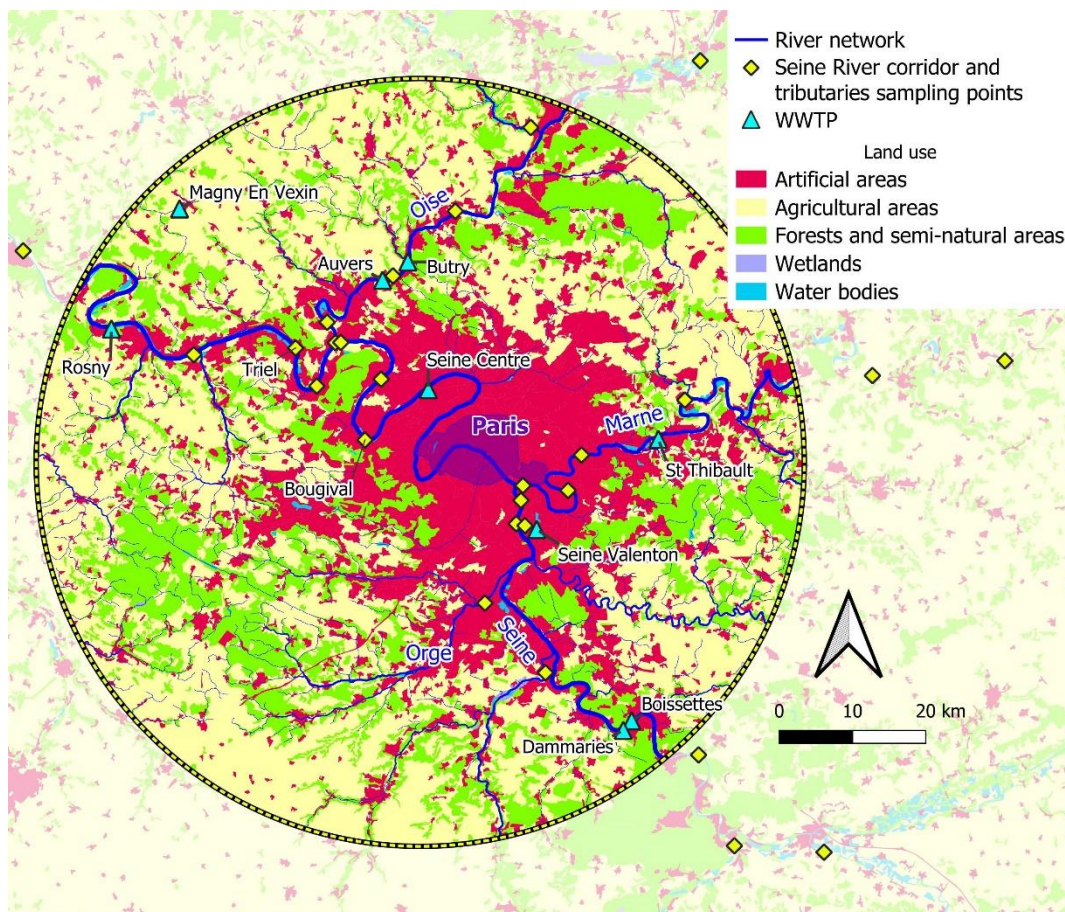
Figure 3: The Orgeval watershed and the sites sampled. Source of land use map: Corine Land Cover 2018, European Union's Copernicus Land Monitoring Service information.



194 **2.3 The Seine River corridor and its tributaries**

195 The sampling sites along the Seine River corridor and its tributaries (Figs. 1 and 4) are representative of
196 different levels of urbanization and anthropogenic pressure on the environment. Two types of samples
197 were collected: river water samples and WWTP discharges. The main sampling sites along the Seine
198 River are Marnay-sur-Seine, Bougival, Triel, and Poses. Marnay-sur-Seine is located some 200 km
199 upstream of Paris (Fig. 1), in La Bassée alluvial plain. Bougival and Triel are located in urban areas (Fig.
200 4): Bougival lies just downstream of Paris and the Seine Centre WWTP, while Triel is located downstream
201 of the Paris metropolitan area, the confluence with the Oise River and the Seine Aval WWTP. Poses is
202 located at the entrance to the Seine estuary (Fig. 1), in a predominantly agricultural area. Other sites were
203 sampled along the Seine River, as well as on some of its major tributaries (Marne and Oise Rivers), and
204 on minor tributaries during specific campaigns.

205 WWTPs of various capacities were also sampled in the Paris region (Fig. 4) to characterize the quality of
206 their treated water in terms of OM. Seven relatively low-capacity WWTPs were selected: Boissette,
207 Dammaries, St. Thibault, Butry, Auvers, Magny en Vexin, and Rosny. Two large-capacity WWTPs
208 managed by the SIAAP (Interdepartmental Syndicate for the Sanitation of Greater Paris) were sampled:
209 Seine Centre and Seine Valenton.



210
211
212
213

Figure 4: Sites sampled along the Seine River corridor and its tributaries: focus on the area around Paris. Source of land use map: Corine Land Cover 2018, European Union's Copernicus Land Monitoring Service information.

214 3 Methodology

215 3.1 The sampling campaigns

216 Several field campaigns were carried out between 2011 and 2024 in the different sites of the Seine River
217 basin. A total of 1047 samples were collected and analyzed, including 178 groundwater samples, 787
218 surface water samples, 23 spring samples, and 59 WWTP effluent samples (Table 1). For all these
219 samples, DOM was characterized both quantitatively (DOC concentration measurement) and
220 qualitatively, through analysis of the optical properties of DOM by optical spectroscopy (UV-Visible



221 absorbance and 3D excitation–emission matrix (EEM) fluorescence spectroscopy). The biodegradable
 222 fraction of DOC (BDOC) was also estimated for 27 % of the samples. Standard physicochemical water
 223 parameters were measured for 45 % of the samples, when possible, to better understand their relationship
 224 with OM properties.

Samples in the database (total: 1047, 27 % with BDOC)								
La Bassée			Orgeval			Seine River corridor and tributaries		
	Samples analyzed	Samples with BDOC		Samples analyzed	Samples with BDOC		Samples analyzed	Samples with BDOC
Alluvial aquifer	75	27 %	Groundwater	62	84 %	Rivers	649	10 %
Chalk aquifer	41	34 %	Rivers	25	80 %	WWTPs	59	92 %
Rivers	46	20 %	Pond	8	100 %			
Oxbow lakes	17	35 %	Agricultural drain	4	100 %			
Gravel pits	38	61 %	Springs	23	48 %			
Total	217	33 %	Total	122	78 %	Total	708	17 %

225 **Table 1: Number of samples collected and analyzed for each geographical unit and type of water. The percentage of samples where**
 226 **the biodegradable fraction of dissolved organic carbon was estimated is also indicated.**

227

228 3.2 Collection and analysis of the water samples

229 Sampling of surface water (rivers, gravel pits, oxbow lakes, ponds, agricultural drains, and springs) was
 230 carried out using a bucket previously rinsed with the respective water to avoid any external pollution.
 231 Groundwater was generally sampled with a 1-L bailer; however, at certain sites in the Orgeval watershed
 232 a peristaltic pump was used because the piezometer opening was obstructed by probes, preventing the use
 233 of a bailer. In all cases, the water level inside the piezometer is first measured, after which the piezometer
 234 is purged and allowed to refill with water before sampling. The sampled water (surface water or
 235 groundwater) is then poured gently into various types of bottles, which are first rinsed well with the same
 236 water, and stored at temperatures between 4°C and 10°C until processing, which occurred on site within
 237 a few minutes to 1 h.



238 Samples from the low-capacity WWTPs were taken by on-site personnel, who collected 2–4 L of treated
239 water from the bottles collected over 24 h using refrigerated samplers. These samples were stored for a
240 few hours in a refrigerator and then transported to the laboratory in a cooler at a temperature below 10°C,
241 where processing occurred within 1–2 h, depending on the distance from the WWTP. In the case of the
242 large-capacity SIAAP WWTPs, samples were obtained by spot sampling to minimize the evolution of
243 OM and its rapidly biodegradable fraction. After sampling, filtration was carried out on site.

244 **3.2.1 Physicochemical water parameters**

245 Measurements of conductivity, pH, dissolved oxygen, and temperature were performed with
246 multiparameter probes directly in the piezometer, after purging, or in the bucket (for surface water and
247 groundwater taken at the pump). Total alkalinity (mmol L^{-1}) was measured on 20 mL of filtered water
248 (GF/F: 0.7 μm) using an automatic titrator (Titrand 905) and HCl (hydrochloric acid, 0.01 M). From
249 several sub-sample analyses (2 to 5) conducted on multiple occasions, we calculated a variation
250 coefficient of 7 %.

251

252 **3.2.2 Dissolved organic carbon and biodegradability**

253 Water samples were filtered immediately after collection through glass fiber filters (Whatman, GF/F,
254 0.7 μm , 25 mm diameter) that had been previously calcined at 450°C for 5 h. DOC analysis was carried
255 out by infrared spectroscopy, after oxidation of the samples using either sodium peroxodisulfate or
256 catalytic combustion, depending on the analysis laboratory.

257 Biodegradability was estimated using the batch incubation method. Filtered samples were re-inoculated
258 with 1 % of non-filtered water and stored in the laboratory at 21°C, in the dark, and with agitation for
259 45 days, during which time the bacteria consumed the OM aerobically (Servais et al., 1999). The
260 biodegradable fraction was then calculated as the difference between DOC content at the end of the
261 incubation period and that at the beginning.

262 The uncertainty associated with the DOC and BDOC concentrations was estimated at 5 % and 10 %,
263 respectively. The uncertainty in DOC concentrations was estimated as the coefficient of variation



264 calculated from quintuplicate analyses of three types of samples: groundwater, river, and pond. Each
265 quintuplicate was incubated for 45 days and sampled three times to estimate BDOC. The uncertainty in
266 BDOC concentrations was estimated as the associated coefficient of variation.

267 **3.2.3 Optical properties of dissolved organic matter**

268 UV-Visible absorbance and EEM fluorescence spectroscopy are rapid, semi-quantitative, and
269 noninvasive techniques that have been widely used for decades (Catalán et al., 2021; Derrien et al., 2019;
270 Huguet et al., 2009; Jaffé et al., 2014; Minor et al., 2014; Parlanti et al., 2000).

271 Immediately after sampling, the water samples were filtered through pyrolyzed (450°C for 1 h) glass fiber
272 filters (Whatman GF/F, 0.7 µm pore size, 25 or 47 mm diameter). The samples were then stored in glass
273 vials at 4°C in the dark until spectroscopic analysis.

274

275 **UV–Visible spectroscopic analysis**

276 UV-Visible absorption spectroscopy was used for rapid determination of the general properties of DOM.
277 Absorbance spectra were recorded (between wavelengths of 210 and 700 nm) using Jasco V-560 and V-
278 760, Aqualog (HORIBA Jobin-Yvon), or UviLine 9400 (Secoman) spectrophotometers. Several indices
279 can be used to obtain information on DOM properties from absorbance spectra. Two indices were retained
280 in the database: the spectral slope ratio (SR) and the SUVA (Specific UV-Absorbance). SR is calculated
281 as the ratio of the absorbance spectrum slope for short wavelengths ($S_{275-295\text{nm}}$) to the spectral slope for
282 longer wavelengths ($S_{350-400\text{nm}}$). The SR ratio is negatively correlated with DOM size: as SR increases the
283 molecular weight decreases (Helms et al., 2008). The SUVA index is calculated as the absorbance at
284 254 nm normalized by the DOC concentration. SUVA is correlated with the percentage of aromaticity of
285 DOM in the aquatic environment. When the SUVA value is high (> 4), DOM is said to be hydrophobic
286 with a strong aromatic character, whereas when it is low (< 3), DOM is said to be hydrophilic (Zsolnay
287 et al., 1999).

288

289 **EEM fluorescence spectroscopy and PARAFAC decomposition**



290 The fluorescence properties of DOM provide information on its structure and general characteristics.
291 Fluorescence is a highly sensitive technique that enables the characterization of DOM from small-volume
292 aqueous samples without the need for concentration or extraction. EEM fluorescence spectroscopy is
293 generally used to characterize DOM and study its dynamics in aquatic environments (Carstea et al., 2010;
294 Ejarque et al., 2017; Huguet et al., 2009; Jaffé et al., 2014; Tzortziou et al., 2015). EEM spectra highlight
295 the various fluorophores constituting DOM and provide information on its source, chemical composition,
296 state of degradation, and reactivity (Ejarque et al., 2017; Fellman et al., 2010; McKnight et al., 2001;
297 Parlanti et al., 2000).

298 Fluorescence spectra were recorded using the Jasco FP-8300, Horiba Jobin-Yvon Aqualog, and Fluorolog
299 FL3-22 spectrofluorometers. Spectra were instrumentally corrected for each instrument and fluorescence
300 intensities were normalized to Raman units. However, the acquisition parameters were not identical across
301 instruments, particularly in terms of the wavelength range and the increments used for excitation and
302 emission. The matrices were therefore homogenized to have common wavelength ranges—250–410 nm
303 at excitation with 10-nm increments, and 260–600 nm at emission with 2-nm increments—so that they
304 could be processed as a whole. The semi-quantitative and qualitative data to be taken into account are the
305 intensity (proportional to fluorophore concentration) and position of fluorescence maxima, which vary
306 according to the nature and origin of the samples and depend on the fluorescent molecular species they
307 contain. Fluorescence indices (humification index [HIX], biological activity index [BIX], and
308 fluorescence index [FI]) are determined in order to characterize the sources and degree of maturation of
309 fluorescent DOM.

310 The HIX (Zsolnay et al., 1999) is used to estimate the degree of aromaticity of DOM. High HIX values
311 ($HIX > 12$) indicate the presence of highly aromatic OM that has undergone transformation or
312 polymerization/polycondensation processes, while low values ($HIX < 4$) indicate a more recent and less
313 aromatic DOM (Huguet et al., 2009). The BIX is used to estimate the presence of freshly produced OM
314 in the environment (Huguet et al., 2009): high values ($BIX > 0.8$) indicate strong biological activity and
315 therefore a recent autochthonous origin (biological or aquatic bacterial) of DOM. The FI (McKnight et
316 al., 2001) identifies the relative contribution of terrestrial ($FI < 1.3$) or microbial ($FI > 1.9$) DOM.

317

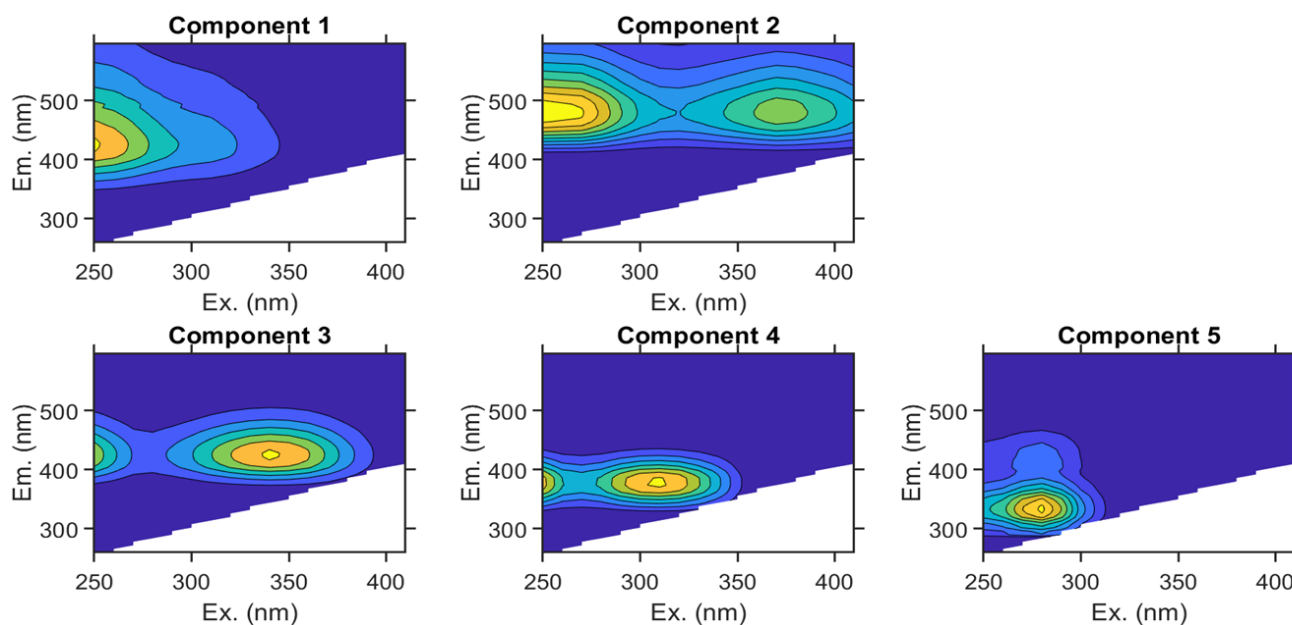


318 All EEM spectra were processed using a multivariate analysis method called "PARAllel FACtor analysis"
319 (PARAFAC), which enables the identification and quantification of fluorophores that vary independently
320 and are referred to as "components." PARAFAC was implemented in Matlab R2021b with the DOMFluor
321 1.7 toolbox. The number of components explaining the overall fluorescence of the whole dataset was
322 determined using split-half analysis (S₄C₄T₂ - Splits: 4, Combinations: 4, Tests: 2) and visual inspection
323 of residuals and component spectra (Murphy et al., 2013).

324

325 This PARAFAC statistical modeling approach allowed us to determine and validate a 5-component model
326 (Fig. 5), explaining 99.5 % of the variability in the entire dataset (1047 samples).

327



328

329

330 **Figure 5. Contour plots of the 5 components determined by PARAFAC.**

331

332 Components C1, C2, C3, C4, and C5 were then compared with those described in the literature and with
333 those recorded in the OpenFluor database (Murphy et al., 2014b), generating matches (Tucker correlation
334 coefficient > 0.95) with the previously reported spectra of 72, 119, 11, 28, and 98 studies, respectively
335 (as of April 2025).



336 Component C1 has been frequently observed in freshwater, forest, and agricultural areas (Calderó-
337 Pascual et al., 2022; Marcé et al., 2021; Stedmon and Markager, 2005) and is attributed to DOM of
338 terrestrial, soil, or plant origin, produced by photo-transformation or microbial degradation (DeFrancesco
339 and Guéguen, 2021; Eder et al., 2022; Moona et al., 2021; Murphy et al., 2014b). This component has
340 been described as corresponding to oxidized quinones (Cory and McKnight, 2005; Groeneveld et al.,
341 2020), a higher proportion of which is possibly due in urban areas to the accumulation of microbe-derived
342 quinones induced by anthropogenic activity (Chai et al., 2019).

343 The literature commonly describes components C2 and C3 as predominantly terrigenous compounds,
344 which are commonly found in freshwater and are generally associated with high-molecular-weight,
345 aromatic, and phenolic materials (DeFrancesco and Guéguen, 2021; Menendez and Tzortziou, 2024;
346 Murphy et al., 2014b; Peleato et al., 2017; Yamashita et al., 2015; Yang et al., 2019).

347 Component C2 corresponds to compounds of terrigenous origin that are commonly found in freshwater
348 and are generally associated with high molecular weights and aromatic material (Dainard et al., 2015;
349 DeFrancesco and Guéguen, 2021; Du et al., 2021; Menéndez and Tzortziou, 2024; Peleato et al., 2017).
350 C2 has been attributed to highly degraded, plant-derived DOM (Podgorski et al., 2018) and reduced
351 quinones of terrestrial origin in forested areas, agricultural watersheds, and wetlands (Cory and
352 McKnight, 2005; Eder et al., 2022; Graeber et al., 2012; Yamashita et al., 2011). Additionally, C2 has
353 been reported as a product or intermediate of the photochemical degradation of terrestrial OM (Eder et
354 al., 2022; Murphy et al., 2014b).

355 Component C3 has a similar emission spectrum to that of a lignin degradation product, syringaldehyde,
356 and has been observed in forested areas (Eder et al., 2022; Murphy et al., 2014b; Peleato et al., 2017).
357 Additionally, it has been found in agricultural areas and nutrient-rich environments, as well as in areas
358 exposed to discharges from WWTPs (Batista-Andrade et al., 2023; Graeber et al., 2012; Jutaporn et al.,
359 2020; Murphy et al., 2011; Yu et al., 2015); it has also been associated with a fluorophore of microbial
360 origin (Maurischat et al., 2022).

361 The fourth component (C4) has been described in the literature as a product of microbial degradation
362 and/or remineralization. It is also associated with biological activity, microbial growth, and algal growth
363 and production (Kurek et al., 2022; Meilleur et al., 2023; Parlanti et al., 2000; Zhuang et al., 2021).



364 However, it has also been linked to anthropogenic sources, such as WWTP effluents (Paradina-Fernández
365 et al., 2023).

366 Component C5 corresponds to protein-like material and is associated with biological activity in the
367 environment (Hambly et al., 2015; Menendez and Tzortziou, 2024; Parlanti et al., 2000; Wunsch and
368 Murphy, 2021). It has been reported as bioavailable DOM in highly productive waters (Gao and Guéguen,
369 2017; Hambly et al., 2015) and in rivers subject to anthropogenic influences (Ouyang et al., 2024).

370

371

372 **4 Description of the dataset**

373 **4.1 Structure of the dataset**

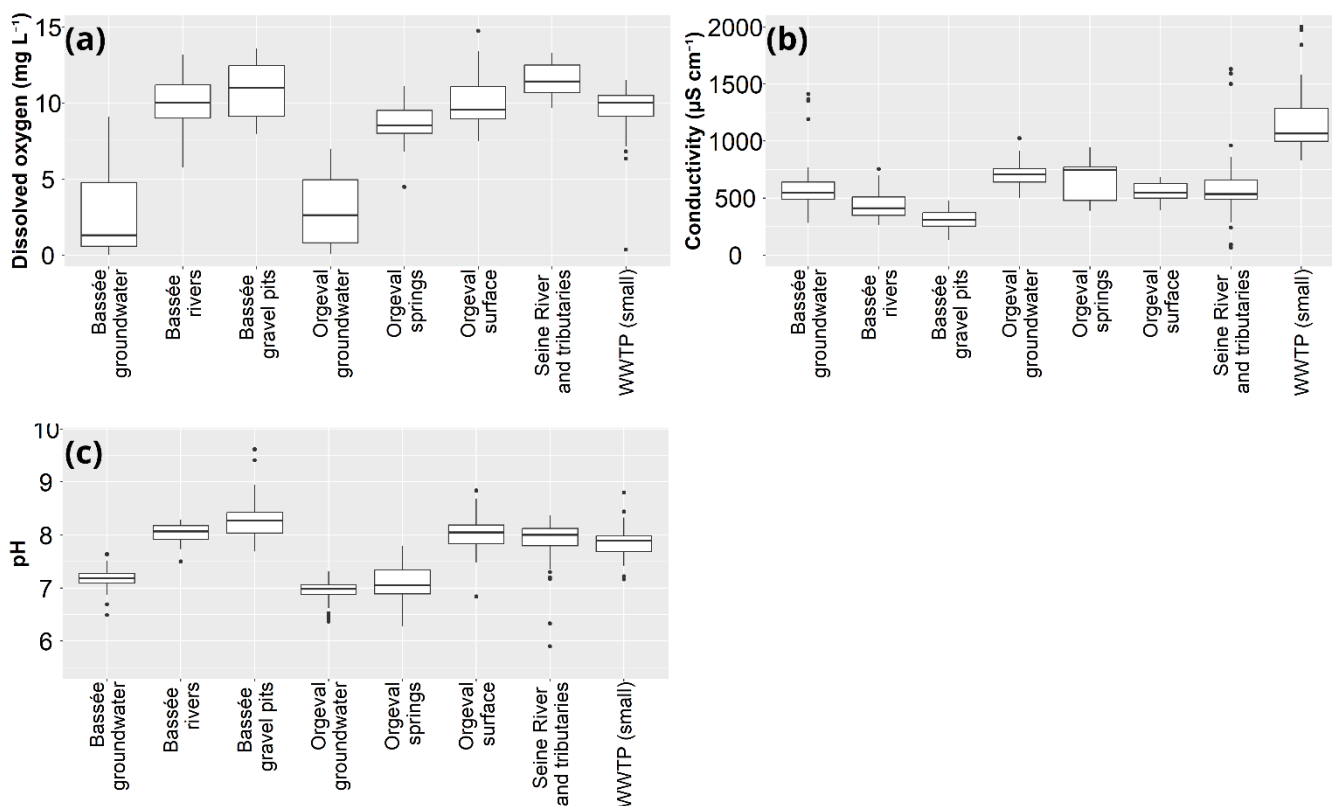
374 The structure of the dataset is thoroughly described in the file “README.pdf”. For each sample, the
375 dataset includes the following variables: temperature, electrical conductivity, pH, dissolved oxygen
376 concentration, alkalinity, concentration of dissolved organic carbon (DOC) and its biodegradable fraction
377 (BDOC), UV-Visible absorbance indices (among them: SUVA (Weishaar et al., 2003) and SR (Helms et
378 al., 2008)), fluorescence indices (HIX (Zsolnay et al., 1999), BIX (Huguet et al., 2009), and FI (McKnight
379 et al., 2001)) and the PARAFAC components (Stedmon and Bro, 2008). For each of the fluorescence
380 spectra of the samples, the excitation-emission matrix is also included.

381 **4.2 General characteristics of dissolved organic matter in the Seine River basin**

382 DOM can be characterized by several variables, such as DOC concentration and the indices derived from
383 spectroscopic analysis: the HIX humification index linked to aromaticity, the BIX biological activity
384 index, the FI index, which discriminates between terrestrial and microbial sources, the SR index linked
385 to OM size, and the SUVA index, associated with aromaticity percentage. Added to these variables are
386 the components determined by the PARAFAC multiway analysis, representing the various fluorophores
387 contributing to the total fluorescence of the sample and of the whole dataset.



388 The physicochemical properties of water, such as dissolved oxygen concentration, conductivity, and pH,
389 can also be studied to better understand their relationship with the properties of DOM.
390 The Seine River basin dataset shows that surface water samples are well oxygenated (around 10 mg L^{-1}),
391 while groundwater is characterized by lower oxygen concentrations ($1\text{--}2.5 \text{ mg L}^{-1}$), particularly in La
392 Bassée alluvial plain, where some samples are almost anoxic (Fig. 6). WWTP discharges have a median
393 conductivity of $1065 \mu\text{S cm}^{-1}$, which is significantly higher than that of natural water samples ($534 \mu\text{S cm}^{-1}$).
394 The conductivity of groundwater is higher than that of surface water, with median values of $609 \mu\text{S cm}^{-1}$
395 and $498 \mu\text{S cm}^{-1}$. pH is close to neutral in groundwater and spring water and is basic in surface water
396 (median 8.0). Particularly high values (up to 9.6) are measured in the gravel pits of La Bassée, due to
397 photosynthesis activity, which consumes CO_2 .



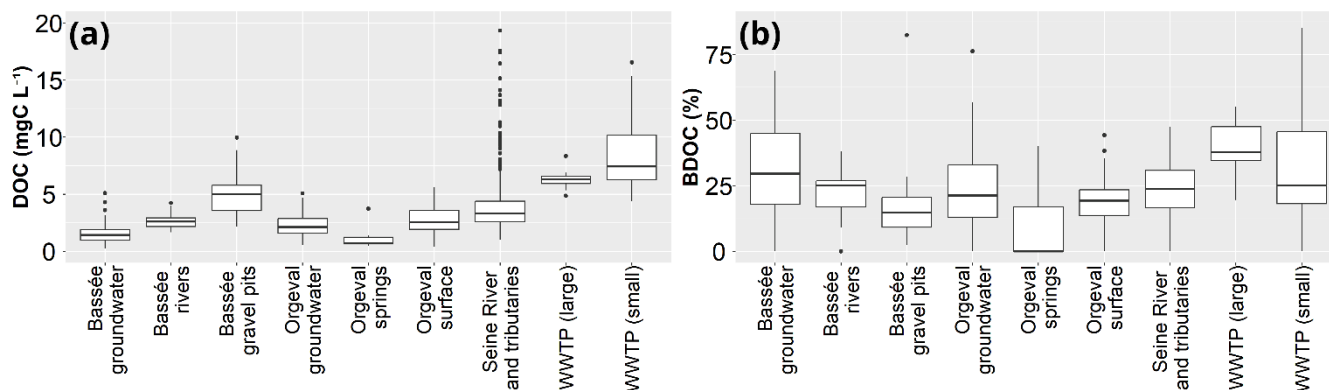
398

399 **Figure 6:** Box plots of the main physicochemical parameters for the different sites and water types: (a) dissolved oxygen; (b)
400 conductivity; (c) pH. The horizontal lines within the boxes indicate the median. The boxes denote the 25th and 75th percentile. The
401 whiskers indicate the minimum and maximum data points, excluding outliers. The points outside the whiskers represent potential
402 outliers.



403 The DOC concentration in the Seine River basin varies depending on the site, the measurement period,
404 and the type of water sampled. Discharges from WWTPs have a higher DOC content than natural waters
405 (median values of 6.8 mgC L^{-1} and 2.9 mgC L^{-1} , respectively) (Fig. 7, Table 2). Overall, concentrations
406 are higher for small-capacity WWTPs than for large-capacity WWTPs. Among natural water samples,
407 surface waters are generally richer in DOC than groundwater is. This is particularly evident in La Bassée
408 alluvial plain, where the median DOC concentrations are 1.4 mgC L^{-1} in aquifers and 2.6 mgC L^{-1} in
409 samples from rivers and oxbows. The numerous gravel pits in La Bassée are particularly rich in DOC
410 (median 5 mgC L^{-1}), as in these water bodies the intense primary production activity is a source of OM.
411 In the Orgeval watershed, DOC values are more similar between surface water and groundwater (Fig. 7,
412 Table 2). This is probably due to the fact that surface water in the Orgeval watershed is represented by
413 small rivers, which are characterized by low primary production. Moreover, this is an essentially
414 agricultural region with few wetlands and therefore few sources of OM, unlike La Bassée alluvial plain.
415 Samples collected from the Seine River and from its tributaries show a wide variability in DOC
416 concentrations (Fig. 7), due to both the diversity of hydrological sampling conditions and the
417 heterogeneity of these samples, ranging from small streams to large rivers.
418 These data shows that the highest DOC concentrations logically occur in WWTP followed by
419 concentrations in surface water, with a high range of values, in the large rivers, possibly receptacles of
420 treated effluents from WWWT. DOC is also high in stagnant system where the organic load is mainly
421 due to algal biomass.

422
423



424

425 **Figure 7: Box plots of (a) the dissolved organic carbon concentration and (b) its biodegradable fraction for the different sites and**
 426 **water types. The horizontal lines within the boxes indicate the median. The boxes denote the 25th and 75th percentile. The whiskers**
 427 **indicate the minimum and maximum data points, excluding outliers. The points outside the whiskers represent potential outliers.**

428

	DOC (mgC L ⁻¹)	BDOC (mgC L ⁻¹)	BDOC/DOC (%)
La Bassée: groundwater	1.4	0.4	30
La Bassée: rivers	2.6	0.5	24
La Bassée: gravel pits	5.0	0.9	15
Orgeval: groundwater	2.1	0.5	21
Orgeval: springs	0.7	undetectable	-
Orgeval: surface water	2.6	0.5	19
Seine River and tributaries	3.4	0.6	25
WWTP (large)	6.3	2.4	38
WWTP (small)	7.6	1.6	25

429

430 **Table 2: Median values for DOC, BDOC, and their ratio.**

431

432 The biodegradable fraction of DOC in the Seine River basin is highly variable, with values ranging from
 433 below the limit of quantification to 85 % (Fig. 7, Table 2). The variability in BDOC among the different
 434 samples is high for each type of water, in particular for WWTPs, for groundwater in La Bassée alluvial
 435 plain and, to a lesser extent, for groundwater of the Orgeval (Fig. 7). This variability is due to the
 436 characteristics of the measurement sites as well as to the hydrological and meteorological conditions of

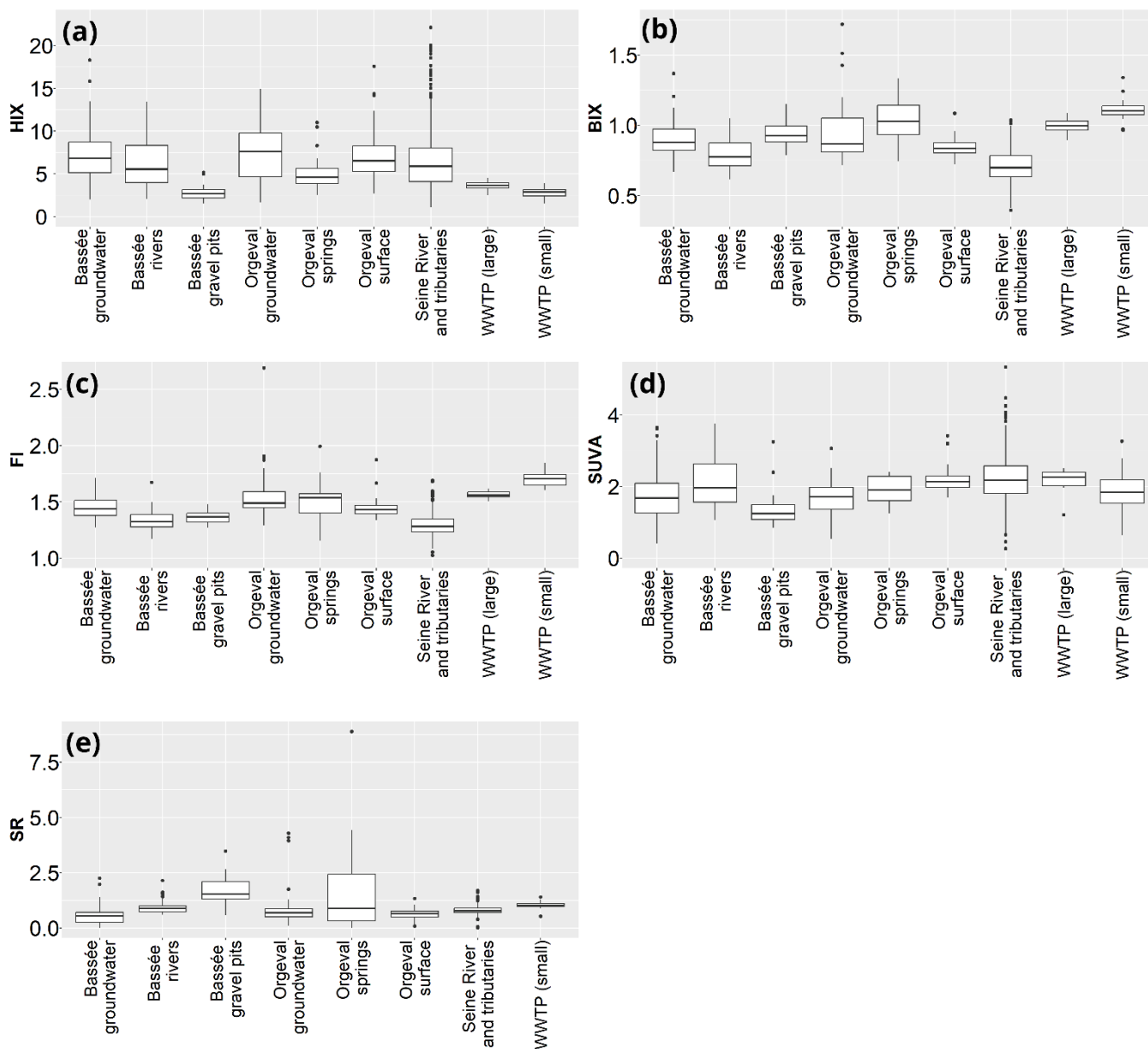


437 the sampling campaigns. DOC inputs from riparian vegetation, or from tree leaf, could be rather
438 biodegradable. It would be interesting to better investigate this variability setting up in situ and/or
439 laboratory experiments. BDOC fractions are generally higher in large-capacity WWTPs (median 38 %)
440 than in small-capacity WWTPs (median 25 %). Natural waters in the basin generally have lower BDOC
441 values (median 21 %), with the exception of groundwater in La Bassée.

442 Specifically, in La Bassée, BDOC fractions are higher in groundwater than in rivers (30 % vs 24 %
443 respectively), and the lowest values are measured in gravel pits (15 %). This configuration could indicate
444 significant bacterial activity in the surface waters of La Bassée, particularly in gravel pits, where much of
445 the produced OM is degraded. Biodegradable fractions in the Orgeval watershed are slightly higher in
446 groundwater than in surface water, which also supports significant bacterial activity (Fig. 7, Table 2). OM
447 in spring water generally contains a lower biodegradable fraction than in other compartments of the Seine
448 hydrosystem. In the Seine River and its tributaries, BDOC fractions range from 0 % to 47 %, with a
449 median of 25 %.

450 DOM in the Seine River basin is relatively low in aromaticity and rather more hydrophilic. Indeed, HIX
451 values are mostly between 3 and 10 for all compartments of the hydrosystem, and the median value in the
452 basin is 5.7 (Fig. 8). This range of HIX values indicates the presence of a significant recent autochthonous
453 contribution of OM. The aromatic character is slightly higher in groundwater (median HIX = 6.9) than in
454 surface water (median HIX = 5.7). La Bassée gravel pits and WWTP discharges are characterized by very
455 low levels of aromatic DOM (median HIX = 2.7 and 3.1, respectively), indicating that the recent
456 autochthonous contribution is particularly significant in these two compartments. Samples collected in
457 the Seine River and in its tributaries show considerable variability in HIX values, as already observed for
458 DOC. BIX values are high for all sites and all water types (Fig.8), revealing high to very high biological
459 activity in all compartments. Biological activity is particularly high in WWTP effluents, especially small-
460 capacity WWTPs (median BIX = 1.1), in the Orgeval springs (BIX = 1), and in groundwater and gravel
461 pits in La Bassée (BIX = 0.9). With the exception of gravel pits, surface waters are characterized by
462 slightly lower BIX than groundwater.

463



464
465
466
467
468
469
470

Figure 8: Box plots of the main indices characterizing DOM by means of optical spectroscopy (UV-Visible absorbance and EEM fluorescence). (a) HIX, humification index; (b) BIX, biological activity index; (c) FI, fluorescence index; (d) SUVA, index, associated with aromaticity percentage; (e) SR, index linked to organic matter size. The horizontal lines within the boxes indicate the median. The boxes denote the 25th and 75th percentile. The whiskers indicate the minimum and maximum data points, excluding outliers. The points outside the whiskers represent potential outliers.



471 The median FI index (Fig. 8) is close to 1.5 for La Bassée and Orgeval groundwater and surface water
472 samples, indicating a mixture of higher plants and microbial sources. Effluents from WWTP are
473 characterized by a more important microbial origin, as indicated by the higher FI values (1.7 median),
474 particularly for small-capacity WWTPs. On the other hand, in the Seine River and its tributaries, the FI
475 indicates a predominantly terrestrial origin (median FI = 1.3). SUVA values are relatively low for
476 groundwater and gravel pits, and slightly higher for river water, spring water, and WWTP effluents.
477 However, most of the values are low (below 3), indicating that DOM is mostly hydrophilic, with a weak
478 aromatic character and a low molecular weight. The smallest molecule sizes (highest SR values) are found
479 in La Bassée gravel pits and in WWTP effluents.

480 These box plots, constructed using simple descriptive statistics, show a typical general trend for DOC and
481 BDOC contents, and highlight the spatio-temporal variability of DOM optical properties in different water
482 bodies in the Seine River watershed. They call for a more in-depth analysis of carbon behavior at the
483 surface water and groundwater interfaces.

484 A principal component analysis was carried out (Fig. 9) with the following variables: conductivity, pH,
485 dissolved oxygen concentration, temperature, DOC, BDOC, HIX, BIX, FI, SUVA, SR, and the relative
486 fluorescence of the five PARAFAC components (expressed as the percentage of fluorescence of each
487 component relative to the sum of the fluorescence intensities of the five components for each sample).

488 The number of individuals was 1047. PCA was performed in R using the FactoMineR and FactoExtra
489 packages. The first plane explains 50 % of the total variability of the dataset. Considering the third axis,
490 the explained variability increases to 60 %.

491 The principal component analysis shows that axis 1 (35 %) is mainly defined in the positive direction by
492 BIX, FI, and the relative fluorescence of component C4, which is of microbial/bacterial type. In the
493 negative direction, axis 1 is defined by the relative fluorescence of components C1 and C2, which are of
494 terrestrial origin, and by the indices HIX and SUVA. This axis therefore seems to be associated with
495 DOM quality: in the positive direction, DOM is autochthonous, freshly produced, degradable, with a
496 strong biological and microbial signature. In the negative direction, DOM is more aromatic, mature,
497 hydrophobic, and of terrestrial origin. Axis 2 (15 %) is mainly represented, in the positive direction, by
498 pH and dissolved oxygen concentration. Data variability seems then to be mainly related to DOM type



499 and to environmental variables (pH and dissolved oxygen), rather than to DOC content and river
500 temperature. These results emphasize the value of this dataset, which encompasses both the quantitative
501 and qualitative characterization of DOM alongside environmental data.

502 WWTP samples are located on the right side in the first plane of the graph of individuals (Fig. 9). They
503 are grouped into two distinct clusters, depending on whether they originate from the effluents of small
504 (Fig. 9b, green asterisks) or large-capacity (Fig. 9b, pink squares) WWTPs. Samples from small-capacity
505 WWTPs are characterized by high biological activity and degradable OM of microbial origin, represented
506 by microbial/bacterial component C4. Samples from large-capacity WWTPs have properties similar to
507 those of certain samples from the Seine and its tributaries: the microbial origin of the OM and the
508 biological activity are lower than for small WWTPs. Gravel pits are well oxygenated, have relatively
509 basic pH values, and contain DOM represented mainly by protein-like compounds characteristic of
510 biological activity (C5). Groundwater is characterized by high conductivity, fairly high biological activity
511 (BIX, FI), and DOM represented mainly by the bacterially/microbially degraded C3 terrestrial
512 component. Samples from the Seine River and its tributaries show OM that is rather aromatic and of
513 terrestrial origin. However, the cloud of observations is quite scattered, indicating that the properties of
514 these samples are highly variable depending on the site and measurement period.

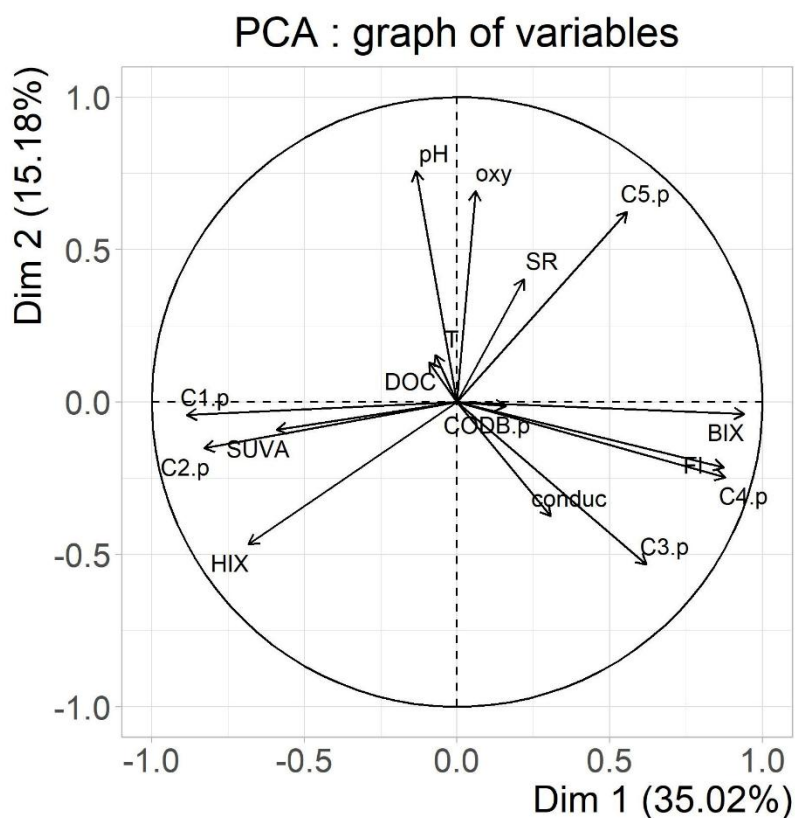
515 To our knowledge, such a dataset, which combines DOC and BDOC concentrations with UV-Visible
516 absorption and EEM/PARAFAC fluorescence properties of DOM, covering a regional watershed over a
517 14-year period, is being proposed to the scientific community for the first time. There is no doubt that due
518 to these widely accessible approaches today, OM characteristics will be made available in other sites than
519 temperate one, giving insights on the microbial processes at work.

520 Overall, the PCA allows us to clearly distinguish between the various types of water in the Seine
521 hydrosystem (surface water, groundwater, WWTP effluent) and geographical units (e.g., La Bassee,
522 Orgeval) and to state that the type of DOM is the main factor affecting the variability of the dataset. PCA
523 analysis is typically recommended for a general overview of data. These data could be further analysed
524 in more detail, perhaps by splitting the dataset into hydrological compartments or seasons, or by adding
525 similar data from other watersheds.

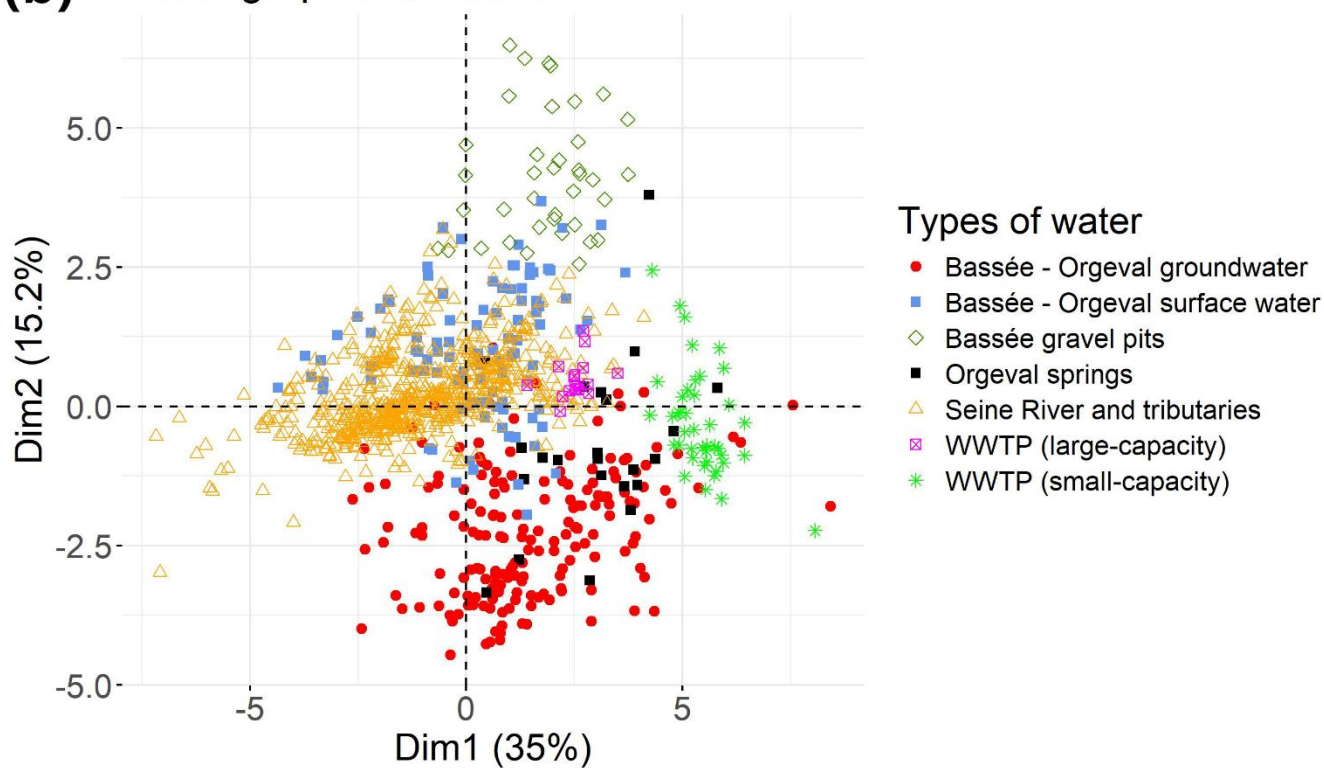
526



(a)



(b) PCA : graph of individuals





528 **Figure 9: Principal component analysis: a) graphs of variables (environmental data (pH, conductivity, dissolved oxygen,**
529 **temperature); DOC content and percentage of biodegradable fraction (CODB.p); HIX, BIX, and FI fluorescence indices; SUVA and**
530 **SR absorbance indices; relative fluorescence (%) of the five components determined by PARAFAC (C1.p to C5.p)) and b) graphs**
531 **of individuals for the first two dimensions.**

532 **Data availability**

533 All data presented in this paper are freely available under the agreement CC BY 4.0 at data.Indores
534 repository: <https://data.indores.fr/privateurl.xhtml?token=a6b58980-3280-4a1b-9311-a0b401955e75>
535 (Baratelli et al., 2025).

536 The dataset consists of the geographic file “Sampling_sites.txt” containing the coordinates and the main
537 characteristics of all the sampling sites; the data file “Data_carbon_Seine_basin.xlsx” containing the
538 variables measured on each sample; a folder with 1047 files with the fluorescence spectra of all the
539 samples; and the metadata file “Metadata_carbon_Seine_basin.xlsx”, which contains the description of
540 all the columns in the data file and in the geographic file.

541 **Conclusions**

542 A dataset is presented to characterize DOM in the Seine River basin both qualitatively and quantitatively.
543 The dataset includes dissolved organic carbon concentrations as well as the results of the analysis of the
544 optical properties of DOM by UV-Visible absorbance and EEM fluorescence spectroscopy. The
545 biodegradable fraction of DOC was also estimated for 27 % of the samples.

546 This dataset is remarkable because water samples were collected from multiple sites across a basin at
547 regional scale, i.e., the Seine River basin in France, which is subject to significant anthropogenic forcing.
548 The sampling sites are representative of different land uses in the Seine River basin and of different
549 compartments of the hydrosystem: surface water, groundwater, and WWTP discharges. Moreover, the
550 dataset covers a 14-year period as well as various hydrological and meteorological conditions.

551 This dataset is available to the scientific community. It can be used to help understand the sources,
552 dynamics, and transformations of OM in the different compartments of a hydrosystem, and particularly
553 at the interface between surface water and groundwater. The influence of various
554 hydrological/meteorological conditions and of the type of site (land use, geology, aquifer residence times)



555 on the DOM characterization can be investigated. These data, measured in the Seine River basin, could
556 serve as a comparison for studies in other regions and to validate new indices characterizing the sources
557 of OM. The dataset can also be used to deepen our understanding of the organic carbon cycle at the
558 regional basin scale, even though studies have already shown that DOC concentrations are about 10 times
559 lower than those of dissolved inorganic carbon (Marescaux et al., 2020; Garnier et al., 2025).
560 Nevertheless, DOM is central for studying river metabolism and additional combined O₂, CO₂, and DOM
561 high-frequency measurements should also offer more in-depth knowledge. In addition to the suggestions
562 provided in the text to encourage the use of this dataset, these observational data could be also used to
563 parameterize and evaluate land-surface models or models assessing the quality of river networks. The
564 model RIVE developed in the framework of the PIREN-Seine program (Billen et al., 1994; Garnier and
565 Billen, 1994; Wang et al., 2024) and describing the biogeochemical processes in aquatic systems is a good
566 candidate for revisiting the DOC-BDOC formalization, using a detailed DOM characterization. This
567 modelling tool `pyRive` is now deposited as a v3.2 version (<https://gitlab.in2p3.fr/rive/pyrive>). The model
568 ProSe-PA (Wang et al., 2022) allowed to improve water quality simulations using a data assimilation
569 technique. Its application at the scale of the Seine River basin pointed out the need of a finer description
570 of the biodegradable component of the organic matter flux at the system's boundary. Our dataset could
571 then contribute to further improve river metabolism simulation with this approach, especially during low
572 flow without algae bloom.
573 The findings from this dataset therefore provide essential information for regional ecosystem modelling,
574 the management of aquatic environments, and restoration strategies that target the impact of human
575 activity on these environments.

576 **Author contribution**

577 Measurements of dissolved organic carbon and its biodegradable fraction were carried out at the METIS
578 laboratory (Sorbonne University) and at LEESU (Paris-Est Créteil University). The investigation of the
579 DOM sources and stages of evolution/degradation was carried out by studying its optical properties at the
580 EPOC laboratory (University of Bordeaux), at LEESU, and at SIAAP (Innovation Department).



581 **Competing interests**

582 The authors declare that they have no conflict of interest.

583 **Acknowledgments**

584 We would like to thank Gwendoline Bourdon, Yuzhe Guo, Zoé Hayet, Benjamin Mercier, Anun Martinez,
585 Romane Nespoulet, Phuong Thanh Nguyen, and Mahaut Sourzac for collecting and/or analyzing water
586 samples.

587 We are grateful to SIAAP, Veolia, Suez, and SAUR for organizing the sampling of the WWTPs and to
588 the MeSeine observatory program (SIAAP) for its help in collecting samples in the Seine Basin. We
589 would also like to thank Jean-Marie Mouchel and Sophie Guillon for contributing to the sampling of some
590 springs in the Orgeval watershed and for providing the coordinates of the sampling sites for the 2018
591 flood campaign. We are also grateful to the farmers in the Orgeval watershed for giving us access to the
592 sampling stations, and to the colleagues at INRAE for giving access to the Boissy experimental station.
593 The PIREN-Seine program (6th, 7th, 8th Phase: <https://piren-seine.fr/>) is greatly acknowledged for its
594 interdisciplinary framework and financial support.

595

596 **References**

- 597 Alvarez-Cobelas, M., Angeler, D. G., Sánchez-Carrillo, S., Almendros, G., 2012. A worldwide view of organic carbon export
598 from catchments. *Biogeochemistry* 107(1), 275–293.
- 599 Artifon, V., Zanardi-Lamardo, E., Fillmann, G., 2019. Aquatic organic matter: Classification and interaction with organic
600 microcontaminants. *Science of the Total Environment* 649, 1620–1635.
- 601 Baratelli, F., Parlanti, E., Garnier, J., Varrault, G., Goffin, A., Musabimana, N., Guérin Rechdaoui, S., Rocher, V., Flipo, N.,
602 2025. Dissolved organic carbon concentrations and optical properties of dissolved organic matter in the Seine River
603 basin. *Data.InDoRES*, <https://data.indores.fr/privateurl.xhtml?token=a6b58980-3280-4a1b-9311-a0b401955e75>.
- 604 Batista-Andrade, J.A., Diaz, E., Iglesias Vega, D., Hain, E., Rose, M.R., Blaney, L., 2023. Spatiotemporal analysis of
605 fluorescent dissolved organic matter to identify the impacts of failing sewer infrastructure in urban streams. *Water*
606 *Research* 229, 119521. <https://doi.org/10.1016/j.watres.2022.119521>
- 607 Battin, T. J., Kaplan, L. A., Findlay, S., Hopkinson, C. S., Marti, E., Packman, A. I., Newbold, J. D., Sabater, F., 2008.
608 Biophysical controls on organic carbon fluxes in fluvial networks. *Nature Geoscience* 1(2), 95–100.
- 609 Battin, T.J., Luysaert, S., Kaplan, L.A., Aufdenkampe, A.K., Richter, A., Tranvik, L.J., 2009. The boundless carbon cycle.
610 *Nature Geosciences* 2, 598–600. <https://doi.org/10.1038/ngeo618>



- 611 Battin, T.J., Lauerwald, R., Bernhardt, E.S., Bertuzzo, E., Gener, L.G., Hall, R.O., Hotchkiss, E.R., Maavara, T., Pavelsky,
612 T.M., Ran, L., Raymond, P., Rosentreter, J.A., Regnier, P., 2023. River ecosystem metabolism and carbon
613 biogeochemistry in a changing world. *Nature* 613, 449–459. <https://doi.org/10.1038/s41586-022-05500-8>
- 614 Bauer, J. E., Bianchi, T. S., 2011. Dissolved Organic Carbon Cycling and Transformation. In *Treatise on Estuarine and Coastal*
615 *Science*, Volume 5, pp. 7–67. Elsevier.
- 616 Besemer, K., Luef, B., Preiner, S., Eichberger, B., Agis, M., Peduzzi, P., 2009. Sources and composition of organic matter for
617 bacterial growth in a large European river floodplain system (Danube, Austria). *Organic Geochemistry* 40(3), 321–
618 331.
- 619 Billen, G., Garnier, J., Hanset, P., 1994. Modelling phytoplankton development in whole drainage networks: the
620 RIVERSTRAHLER model applied to the Seine River system. *Hydrobiologia* (289), 119–137.
621 https://doi.org/10.1007/978-94-017-2670-2_11.
- 622 Billen, G., Garnier, J., Mouchel, J.-M., Silvestre, M., 2007. The Seine system: Introduction to a multidisciplinary approach of
623 the functioning of a regional river system. *Science of The Total Environment*, Human activity and material fluxes in
624 a regional river basin: the Seine River watershed 375, 1–12. <https://doi.org/10.1016/j.scitotenv.2006.12.001>
- 625 Calderó-Pascual, M., Yıldız, D., Yalçın, G., Metin, M., Yetim, S., Fiorentin, C., Andersen, M.R., Jennings, E., Jeppesen, E.,
626 Ger, K.A., Beklioglu, M., McCarthy, V., 2022. The importance of allochthonous organic matter quality when
627 investigating pulse disturbance events in freshwater lakes: a mesocosm experiment. *Hydrobiologia* 849, 3905–3929.
- 628 Carlson, C.A., Hansell, D.A., 2015. DOM Sources, Sinks, Reactivity, and Budgets, in: *Biogeochemistry of Marine Dissolved*
629 *Organic Matter*. Elsevier, pp. 65–126. <https://doi.org/10.1016/B978-0-12-405940-5.00003-0>
- 630 Carstea, E.M., Baker, A., Bieroza, M., Reynolds, D., 2010. Continuous fluorescence excitation–emission matrix monitoring
631 of river organic matter. *Water Res* 44, 5356–5366.
- 632 Catalán, N., Pastor, A., Borrego, C.M., Casas-Ruiz, J.P., Hawkes, J.A., Gutiérrez, C., Schiller, D., Marcé, R., 2021. The
633 relevance of environment vs. composition on dissolved organic matter degradation in freshwaters. *Limnol Oceanogr*
634 66, 306–320.
- 635 Cawley, K. M., Butler, K. D., Aiken, G. R., Larsen, L. G., Huntington, T. G., McKnight, D. M., 2012. Identifying fluorescent
636 pulp mill effluent in the Gulf of Maine and its watershed. *Marine Pollution Bulletin* 64(8), 1678–1687.
- 637 Chai, L., Huang, M., Fan, H., Wang, J., Jiang, D., Zhang, M., Huang, Y., 2019. Urbanization altered regional soil organic
638 matter quantity and quality: Insight from excitation emission matrix (EEM) and parallel factor analysis (PARAFAC).
639 *Chemosphere* 220, 249–258.
- 640 Cole, J.J., Prairie, Y.T., Caraco, N.F., McDowell, W.H., Tranvik, L.J., Striegl, R.G., Duarte, C.M., Kortelainen, P., Downing,
641 J.A., Middelburg, J.J., Melack, J., 2007. Plumbing the Global Carbon Cycle: Integrating Inland Waters into the
642 Terrestrial Carbon Budget. *Ecosystems* 10, 172–185. <https://doi.org/10.1007/s10021-006-9013-8>
- 643 Cory, R. M., McKnight, D. M., 2005. Fluorescence spectroscopy reveals ubiquitous presence of oxidized and reduced quinones
644 in dissolved organic matter. *Environmental Science & Technology* 39(21), 8142–8149.
- 645 Cory, R. M., Boyer, E. W., McKnight, D. M., 2011. *Spectral Methods to Advance Understanding of Dissolved Organic Carbon*
646 *Dynamics in Forested Catchments*, pp. 117–135. Dordrecht: Springer Netherlands.
- 647 Dainard, P.G., Guéguen, C., McDonald, N., Williams, W.J., 2015. Photobleaching of fluorescent dissolved organic matter in
648 Beaufort Sea and North Atlantic Subtropical Gyre. *Marine Chemistry* 177, 630–637.
- 649 DeFrancesco, C., Guéguen, C., 2021. Long-term trends in dissolved organic matter composition and its relation to sea ice in
650 the Canada Basin, Arctic Ocean (2007–2017). *Journal of Geophysical Research: Oceans* 126(2).
- 651 Derrien, M., Brogi, S.R., Gonçalves-Araujo, R., 2019. Characterization of aquatic organic matter: Assessment, perspectives
652 and research priorities. *Water Research* 163, 114908. <https://doi.org/10.1016/j.watres.2019.114908>
- 653 Drake, T.W., Raymond, P.A., Spencer, R.G.M., 2018. Terrestrial carbon inputs to inland waters: A current synthesis of
654 estimates and uncertainty. *Limnology and Oceanography Letters* 3, 132–142. <https://doi.org/10.1002/lo2.10055>
- 655 Du, Y., Lu, Y., Roebuck, J.A., Liu, D., Chen, F., Zeng, Q., Xiao, K., He, H., Liu, Z., Zhang, Y., Jaffé, R., 2021. Direct versus
656 indirect effects of human activities on dissolved organic matter in highly impacted lakes. *Science of The Total*
657 *Environment* 752, 141839.
- 658 Eder, A., Weigelhofer, G., Pucher, M., Tiefenbacher, A., Strauss, P., Brandl, M., Blöschl, G., 2022. Pathways and composition
659 of dissolved organic carbon in a small agricultural catchment during base flow conditions. *Ecohydrology &*
660 *Hydrobiology* 22, 96–112.



- 661 Ejarque, E., Freixa, A., Vazquez, E., Guarch, A., Amalfitano, S., Fazi, S., Romaníe, A.M., Butturini, A., 2017. Quality and
662 reactivity of dissolved organic matter in a Mediterranean river across hydrological and spatial gradients. *Science of*
663 *the Total Environment* 599–600, 1802–1812.
- 664 Fellman, J.B., Hood, E., Spencer, R.G.M., 2010. Fluorescence spectroscopy opens new windows into dissolved organic matter
665 dynamics in freshwater ecosystems: A review. *Limnol. Oceanogr* 55, 2452–2462.
- 666 Flipo, N., Labadie, P., Lestel, L. (Eds.), 2021. *The Seine River Basin, The Handbook of Environmental Chemistry*. Springer
667 International Publishing, Cham. <https://doi.org/10.1007/978-3-030-54260-3>
- 668 Floury, P., Gaillardet, J., Tallec, G., Ansart, P., Bouchez, J., Louvat, P., Gorge, C., 2019. Chemical weathering and CO₂
669 consumption rate in a multilayered-aquifer dominated watershed under intensive farming: The Orgeval Critical Zone
670 Observatory, France. *Hydrological Processes* 33, 195–213. <https://doi.org/10.1002/hyp.13340>
- 671 Friedlingstein, P., O’Sullivan, M., Jones, M.W., Andrew, R.M., Bakker, D.C.E., Hauck, J., Landschützer, P., Le Quéré, C.,
672 Luijkx, I.T., Peters, G.P., Peters, W., Pongratz, J., Schwingshackl, C., Sitch, S., Canadell, J.G., Ciais, P., Jackson,
673 R.B., Alin, S.R., Anthoni, P., Barbero, L., Bates, N.R., Becker, M., Bellouin, N., Decharme, B., Bopp, L., Brasika,
674 I.B.M., Cadule, P., Chamberlain, M.A., Chandra, N., Chau, T.-T.-T., Chevallier, F., Chini, L.P., Cronin, M., Dou, X.,
675 Enyo, K., Evans, W., Falk, S., Feely, R.A., Feng, L., Ford, D.J., Gasser, T., Ghattas, J., Gkritzalis, T., Grassi, G.,
676 Gregor, L., Gruber, N., Gürses, Ö., Harris, I., Hefner, M., Heinke, J., Houghton, R.A., Hurtt, G.C., Iida, Y., Ilyina,
677 T., Jacobson, A.R., Jain, A., Jarníková, T., Jersild, A., Jiang, F., Jin, Z., Joos, F., Kato, E., Keeling, R.F., Kennedy,
678 D., Klein Goldewijk, K., Knauer, J., Korsbakken, J.I., Körtzinger, A., Lan, X., Lefèvre, N., Li, H., Liu, J., Liu, Z.,
679 Ma, L., Marland, G., Mayot, N., McGuire, P.C., McKinley, G.A., Meyer, G., Morgan, E.J., Munro, D.R., Nakaoka,
680 S.-I., Niwa, Y., O’Brien, K.M., Olsen, A., Omar, A.M., Ono, T., Paulsen, M., Pierrot, D., Pockock, K., Poulter, B.,
681 Powis, C.M., Rehder, G., Resplandy, L., Robertson, E., Rödenbeck, C., Rosan, T.M., Schwinger, J., Séférian, R.,
682 Smallman, T.L., Smith, S.M., Sospedra-Alfonso, R., Sun, Q., Sutton, A.J., Sweeney, C., Takao, S., Tans, P.P., Tian,
683 H., Tilbrook, B., Tsujino, H., Tubiello, F., Van Der Werf, G.R., Van Ooijen, E., Wanninkhof, R., Watanabe, M.,
684 Wimart-Rousseau, C., Yang, D., Yang, X., Yuan, W., Yue, X., Zaehle, S., Zeng, J., Zheng, B., 2023. *Global Carbon*
685 *Budget 2023*. *Earth Syst. Sci. Data* 15, 5301–5369. <https://doi.org/10.5194/essd-15-5301-2023>
- 686 Gaillardet, J., Braud, I., Hankard, F., Anquetin, S., Bour, O., Dorfliger, N., de Dreuzy, J. r., Galle, S., Galy, C., Gogo, S.,
687 Gourcy, L., Habets, F., Laggoun, F., Longuevergne, L., Le Borgne, T., Naaïm-Bouvet, F., Nord, G., Simonneaux, V.,
688 Six, D., Tallec, T., Valentin, C., Abril, G., Allemand, P., Arènes, A., Arfib, B., Arnaud, L., Arnaud, N., Arnaud, P.,
689 Audry, S., Comte, V.B., Batiot, C., Battais, A., Bellot, H., Bernard, E., Bertrand, C., Bessière, H., Binet, S., Bodin,
690 J., Bodin, X., Boithias, L., Bouchez, J., Boudevillain, B., Moussa, I.B., Branger, F., Braun, J.J., Brunet, P., Caceres,
691 B., Calmels, D., Cappelaere, B., Celle-Jeanton, H., Chabaux, F., Chalikakis, K., Champollion, C., Copard, Y., Cotel,
692 C., Davy, P., Deline, P., Delrieu, G., Demarty, J., Dessert, C., Dumont, M., Emblanch, C., Ezzahar, J., Estèves, M.,
693 Favier, V., Fauchoux, M., Filizola, N., Flammarion, P., Floury, P., Fovet, O., Fournier, M., Francez, A.J., Gandois,
694 L., Gascuel, C., Gayer, E., Genthon, C., Gérard, M.F., Gilbert, D., Gouttevin, I., Grippa, M., Gruau, G., Jardani, A.,
695 Jeanneau, L., Join, J.L., Jourde, H., Karbou, F., Labat, D., Lagadeuc, Y., Lajeunesse, E., Lastennet, R., Lavado, W.,
696 Lawin, E., Lebel, T., Le Bouteiller, C., Legout, C., Lejeune, Y., Le Meur, E., Le Moigne, N., Lions, J., Lucas, A.,
697 Malet, J.P., Marais-Sicre, C., Maréchal, J.C., Marlin, C., Martin, P., Martins, J., Martinez, J.M., Massei, N., Mauclerc,
698 A., Mazzilli, N., Molénat, J., Moreira-Turcq, P., Mougín, E., Morin, S., Ngoupayou, J.N., Panthou, G., Peugeot, C.,
699 Picard, G., Pierret, M.C., Porel, G., Probst, A., Probst, J.L., Rabatel, A., Raclot, D., Ravanel, L., Rejiba, F., René, P.,
700 Ribolzi, O., Riotte, J., Rivière, A., Robain, H., Ruiz, L., Sanchez-Perez, J.M., Santini, W., Sauvage, S., Schoeneich,
701 P., Seidel, J.L., Sekhar, M., Sengtaeuanghoung, O., Silvera, N., Steinmann, M., Soruco, A., Tallec, G., Thibert, E.,
702 Lao, D.V., Vincent, C., Viville, D., Wagnon, P., Zitouna, R., 2018. OZCAR: The French Network of Critical Zone
703 Observatories. *Vadose Zone Journal* 17, 180067. <https://doi.org/10.2136/vzj2018.04.0067>
- 704 Gao, Z., Guéguen, C., 2017. Size distribution of absorbing and fluorescing DOM in Beaufort Sea, Canada Basin. *Deep Sea*
705 *Research Part I: Oceanographic Research Papers* 121, 30–37. <https://doi.org/10.1016/j.dsr.2016.12.014>
- 706 Garnier, J., Billen, G., 1994. Ecological interactions in a shallow sand-pit lake (Lake Créteil, Parisian Basin, France): a
707 modelling approach. *Hydrobiologia* 275/276, 97–114. https://doi.org/10.1007/978-94-017-2460-9_9
- 708 Garnier, J., Billen, G., Vilain, G., Benoit, M., Passy, P., Tallec, G., Tournebize, J., Anglade, J., Billy, C., Mercier, B., Ansart,
709 P., Azougui, A., Sebilo, M., Kao, C., 2014. Curative vs. preventive management of nitrogen transfers in rural areas:



- 710 Lessons from the case of the Orgeval watershed (Seine River basin, France). *Journal of Environmental Management*
711 144, 125–134. <https://doi.org/10.1016/j.jenvman.2014.04.030>
- 712 Garnier, J., Guillon, S., Hénine, H., Billen, G., Escoffier, N., Mercier, B., Martinez A., Mouchel, J. M., 2025. Sources and fate
713 of CO₂ along the soil–aquifer–stream–atmosphere continuum (the Orgeval headwater catchment, France). *Geoderma*,
714 458, 117297. <https://doi.org/10.1016/j.geoderma.2025.117297>
- 715 Graeber, D., Gelbrecht, J., Pusch, M.T., Anlanger, C., Von Schiller, D., 2012. Agriculture has changed the amount and
716 composition of dissolved organic matter in Central European headwater streams. *Science of The Total Environment*
717 438, 435–446.
- 718 Groeneveld, M., Catalán, N., Attermeyer, K., Hawkes, J., Einarsdóttir, K., Kothawala, D., Bergquist, J., Tranvik, L., 2020.
719 Selective Adsorption of Terrestrial Dissolved Organic Matter to Inorganic Surfaces Along a Boreal Inland Water
720 Continuum. *JGR Biogeosciences* 125, e2019JG005236.
- 721 Hambly, A.C., Arvin, E., Pedersen, L.-F., Pedersen, P.B., Sereďyńska-Sobecka, B., Stedmon, C.A., 2015. Characterising
722 organic matter in recirculating aquaculture systems with fluorescence EEM spectroscopy. *Water Research* 83, 112–
723 120. <https://doi.org/10.1016/j.watres.2015.06.037>
- 724 Helms, J.R., Stubbins, A., Ritchie, J.D., Minor, E.C., Kieber, D.J., Mopper, K., 2008. Absorption spectral slopes and slope
725 ratios as indicators of molecular weight, source, and photobleaching of chromophoric dissolved organic matter.
726 *Limnol. Oceanogr* 53, 955–969.
- 727 Huguet, A., Vacher, L., Relexans, S., Saubusse, S., Froidefond, J.-M., Parlanti, E., 2009. Properties of fluorescent dissolved
728 organic matter in the Gironde Estuary. *Org. Geochem* 40, 706.
- 729 Jaffé, R., McKnight, D., Maie, N., Cory, R., McDowell, W.H., Campbell, J.L., 2008. Spatial and temporal variations in DOM
730 composition in ecosystems: The importance of long-term monitoring of optical properties. *J. Geophys. Res.* 113,
731 2008JG000683.
- 732 Jaffé, R., Cawley, K.M., Yamashita, Y., 2014. Applications of Excitation Emission Matrix Fluorescence with Parallel Factor
733 Analysis (EEM-PARAFAC) in Assessing Environmental Dynamics of Natural Dissolved Organic Matter (DOM) in
734 Aquatic Environments: A Review. *Advances in the Physicochemical Characterization of Dissolved Organic Matter:
735 Impact on Natural and Engineered Systems*. Chapter 3, 27–73.
- 736 Jutaporn, P., Armstrong, M.D., Coronell, O., 2020. Assessment of C-DBP and N-DBP formation potential and its reduction
737 by MIEX® DOC and MIEX® GOLD resins using fluorescence spectroscopy and parallel factor analysis. *Water
738 Research* 172, 115460. <https://doi.org/10.1016/j.watres.2019.115460>
- 739 Kurek, M.R., Frey, K.E., Guillemette, F., Podgorski, D.C., Townsend-Small, A., Arp, C.D., Kellerman, A.M., Spencer,
740 R.G.M., 2022. Trapped Under Ice: Spatial and Seasonal Dynamics of Dissolved Organic Matter Composition in
741 Tundra Lakes. *JGR Biogeosciences* 127, e2021JG006578. <https://doi.org/10.1029/2021JG006578>
- 742 Lambert, T., Bouillon, S., Darchambeau, F., Morana, C., Roland, F. A. E., Descy, J. P., Borges, A. V., 2017. Effects of human
743 land use on the terrestrial and aquatic sources of fluvial organic matter in a temperate river basin (The Meuse River,
744 Belgium). *Biogeochemistry* 136.
- 745 Lestel, L., Eschbach, D., Steinmann, R., Gastaldi, N., 2018. *ArchiSEINE : une approche géohistorique du bassin de la Seine*,
746 Fascicule #18 du PIREN-Seine, ISBN : 978-2-490463-07-7, ARCEAU-IdF, 64 p.
- 747 McKnight, D.M., Boyer, E.W., Westerhoff, P.K., Doran, P.T., Kulbe, T., Andersen, D.T., 2001. Spectrofluorometric
748 characterization of dissolved organic matter for indication of precursor organic material and aromaticity. *Limnol.
749 Oceanogr* 46, 38–48.
- 750 Marcé, R., Verdura, L., Leung, N., 2021. Dissolved organic matter spectroscopy reveals a hot spot of organic matter changes
751 at the river–reservoir boundary. *Aquat Sci* 83, 67.
- 752 Marescaux, A., Thieu, V., Gypens, N., Silvestre, M., Garnier, J., 2020. Modeling inorganic carbon dynamics in the Seine River
753 continuum in France. *Hydrology and Earth System Sciences*, 24(5), 2379–2398. [https://doi.org/10.5194/hess-24-
754 2379-2020](https://doi.org/10.5194/hess-24-2379-2020)
- 755 Maurischat, P., Lehnert, L., Zerres, V.H.D., Tran, T.V., Kalbitz, K., Rinnan, Å., Li, X.G., Dorji, T., Guggenberger, G., 2022.
756 The glacial–terrestrial–fluvial pathway: A multiparametrical analysis of spatiotemporal dissolved organic matter
757 variation in three catchments of Lake Nam Co, Tibetan Plateau. *Science of The Total Environment* 838, 156542.
758 <https://doi.org/10.1016/j.scitotenv.2022.156542>



- 759 Meilleur, C., Kamula, M., Kuzyk, Z.A., Guéguen, C., 2023. Insights into surface circulation and mixing in James Bay and
760 Hudson Bay from dissolved organic matter optical properties. *Journal of Marine Systems* 238, 103841.
- 761 Menendez, A., Tzortziou, M., 2024. Driving factors of colored dissolved organic matter dynamics across a complex urbanized
762 estuary. *Science of The Total Environment* 921, 171083. <https://doi.org/10.1016/j.scitotenv.2024.171083>
- 763 Minor, E.C., Swenson, M.M., Mattson, B.M., Oyler, A.R., 2014. Structural characterization of dissolved organic matter: a
764 review of current techniques for isolation and analysis. *Environ. Sci.: Processes Impacts* 16, 2064–2079.
765 <https://doi.org/10.1039/C4EM00062E>
- 766 Moona, N., Holmes, A., Wunsch, U. J., Pettersson, T. J. R., Murphy, K. R., 2021. Full-scale manipulation of the empty bed
767 contact time to optimize dissolved organic matter removal by drinking water biofilters. *ACS ES&T Water* 1(5), 1117–
768 1126.
- 769 Mouhri, A., Flipo, N., Rejiba, F., de Fouquet, C., Bodet, L., Kurtulus, B., Tallec, G., Durand, V., Jost, A., Ansart, P., Goblet,
770 P., 2013. Designing a multi-scale sampling system of stream–aquifer interfaces in a sedimentary basin. *Journal of*
771 *Hydrology* 504, 194–206. <https://doi.org/10.1016/j.jhydrol.2013.09.036>
- 772 Murphy, K.R., Hambly, A., Singh, S., Henderson, R.K., Baker, A., Stuetz, R., Khan, S.J., 2011. Organic Matter Fluorescence
773 in Municipal Water Recycling Schemes: Toward a Unified PARAFAC Model. *Environ. Sci. Technol.* 45, 2909–2916.
774 <https://doi.org/10.1021/es103015e>
- 775 Murphy, K. R., Stedmon, C. A., Graeber, D., Bro, R., 2013. Fluorescence spectroscopy and multi-way techniques. *PARAFAC.*
776 *Analytical Methods* 5(23), 6557.
- 777 Murphy, K.R., Bro, R., Stedmon, C.A., 2014a. Chemometric Analysis of Organic Matter Fluorescence, in: Coble, P.G., Lead,
778 J., Baker, A., Reynolds, D.M., Spencer, R.G.M. (Eds.), *Aquatic Organic Matter Fluorescence*. Cambridge University
779 Press, pp. 339–375.
- 780 Murphy, K.R., Stedmon, C.A., Wenig, P., Bro, R., 2014b. OpenFluor– an online spectral library of auto-fluorescence by
781 organic compounds in the environment. *Anal. Methods* 6, 658.
- 782 Ouyang, T., McKenna, A.M., Wozniak, A.S., 2024. Storm-driven hydrological, seasonal, and land use/land cover impact on
783 dissolved organic matter dynamics in a mid-Atlantic, USA coastal plain river system characterized by 21 T FT-ICR
784 mass spectrometry. *Front. Environ. Sci.* 12, 1379238. <https://doi.org/10.3389/fenvs.2024.1379238>
- 785 Paradina-Fernández, L., Wunsch, U., Bro, R., Murphy, K., 2023. Direct Measurement of Organic Micropollutants in Water
786 and Wastewater Using Fluorescence Spectroscopy. *ACS EST Water* 3, 3905–3915.
787 <https://doi.org/10.1021/acsestwater.3c00323>
- 788 Parlanti, E., Worz, K., Geoffroy, L., Lamotte, M., 2000. Dissolved organic matter fluorescence spectroscopy as a tool to
789 estimate biological activity in a coastal zone submitted to anthropogenic inputs. *Org. Geochem* 31, 1765–1781.
- 790 Peleato, N. M., Sidhu, B. S., Legge, R. L., Andrews, R. C., 2017. Investigation of ozone and peroxone impacts on natural
791 organic matter character and biofiltration performance using fluorescence spectroscopy. *Chemosphere* 172, 225–233.
- 792 Podgorski, D.C., Zito, P., McGuire, J.T., Martinovic-Weigelt, D., Cozzarelli, I.M., Bekins, B.A., Spencer, R.G.M., 2018.
793 Examining Natural Attenuation and Acute Toxicity of Petroleum-Derived Dissolved Organic Matter with Optical
794 Spectroscopy. *Environ. Sci. Technol.* 52, 6157–6166. <https://doi.org/10.1021/acs.est.8b00016>
- 795 Raymond, P.A., Hartmann, J., Lauerwald, R., Sobek, S., McDonald, C., Hoover, M., Butman, D., Striegl, R., Mayorga, E.,
796 Humborg, C., Kortelainen, P., Dürr, H., Meybeck, M., Ciais, P., Guth, P., 2013. Global carbon dioxide emissions
797 from inland waters. *Nature* 503, 355–359. <https://doi.org/10.1038/nature12760>
- 798 Regnier, P., Resplandy, L., Najjar, R.G., Ciais, P., 2022. The land-to-ocean loops of the global carbon cycle. *Nature* 603, 401–
799 410. <https://doi.org/10.1038/s41586-021-04339-9>
- 800 Servais, P., Garnier, J., Demarteau, N., Brion, N., Billen, G., 1999. Supply of organic matter and bacteria to aquatic ecosystems
801 through waste water effluents. *Water Research* 33, 3521–3531. [https://doi.org/10.1016/S0043-1354\(99\)00056-1](https://doi.org/10.1016/S0043-1354(99)00056-1)
- 802 Stedmon, C. A., Markager, S., 2005. Resolving the variability in dissolved organic matter fluorescence in a temperate estuary
803 and its catchment using PARAFAC analysis. *Limnology and Oceanography* 50(2), 686–697.
- 804 Stedmon, C., Bro, R., 2008. Characterizing dissolved organic matter fluorescence with parallel factor analysis: a tutorial.
805 *Limnol. Ocean. Methods* 6, 572–579.
- 806 Tusseau-Vuillemin, M. H., Le Reveillé, G., 2001. Le carbone organique biodégradable dans les eaux traitées des stations
807 d'épuration du bassin de la seine. *Ingénieries eau-agriculture-territoires* 25, 3–12.



- 808 Tzortziou, M., Zeri, C., Dimitriou, E., Ding, Y., Jaffé, R., Anagnostou, E., Pitta, E., Mentzafou, A., 2015. Colored dissolved
809 organic matter dynamics and anthropogenic influences in a major transboundary river and its coastal wetland. *Limnol.*
810 *Oceanogr* 60, 1222–1240.
- 811 Wang, S., Flipo, N., Romary, T., Hasanyar, M., 2022. Particle filter for high frequency oxygen data assimilation in river
812 systems. *Environmental Modelling & Software*, 151:105382. ISSN 1364-8152.
813 <https://doi.org/10.1016/j.envsoft.2022.105382>
- 814 Wang, S., Thieu, V., Billen, G., Garnier, J., Silvestre, M., Marescaux, A., Yan, X., Flipo, N., 2024. The community-centered
815 freshwater biogeochemistry model unified RIVE v1. 0: a unified version for water column. *Geoscientific Model*
816 *Development*, 17(1), 449-476. <https://doi.org/10.5194/gmd-17-449-2024>
- 817 Weishaar, G., Aiken, R., Bergamschi, B.A., Fram, M.S., Fugii, R., Mopper, K. 2003. Evaluation of Specific Ultraviolet
818 Absorbance as an Indicator of the Chemical Composition and Reactivity of Dissolved Organic Carbon.
819 *Environmental Science and Technology*, 37(20), 4702-4708, doi:10.1021/es030360x.
- 820 Wiegner, T. N., Tubal, R. L., MacKenzie, R.A., 2009. Bioavailability and export of dissolved organic matter from a tropical
821 river during base- and stormflow conditions. *Limnology and Oceanography*, 54(4):1233–1242. ISSN 00243590. doi:
822 10.4319/lo.2009.54.4.1233.
- 823 Wünsch, U.J., Murphy, K., 2021. A simple method to isolate fluorescence spectra from small dissolved organic matter datasets.
824 *Water Research* 190, 116730. <https://doi.org/10.1016/j.watres.2020.116730>
- 825 Yamashita, Y., Kloeppel, B.D., Knoepp, J., Zausen, G.L., Jaffé, R., 2011. Effects of Watershed History on Dissolved Organic
826 Matter Characteristics in Headwater Streams. *Ecosystems* 14, 1110–1122.
- 827 Yan, Y., Lauerwald, R., Wang, X., Regnier, P., Ciais, P., Ran, L., Gao, Y., Huang, L., Zhang, Y., Duan, Z., Papa, F., Yu, B.,
828 Piao, S., 2023. Increasing riverine export of dissolved organic carbon from China. *Global Change Biology* 29, 5014–
829 5032. <https://doi.org/10.1111/gcb.16819>
- 830 Yang, L., Chen, W., Zhuang, W.-E., Cheng, Q., Li, W., Wang, H., Guo, W., Chen, C.-T.A., Liu, M., 2019. Characterization
831 and bioavailability of rainwater dissolved organic matter at the southeast coast of China using absorption spectroscopy
832 and fluorescence EEM-PARAFAC. *Estuarine, Coastal and Shelf Science* 217, 45–55.
833 <https://doi.org/10.1016/j.ecss.2018.11.002>
- 834 Yu, H., Liang, H., Qu, F., Han, Z., Shao, S., Chang, H., Li, G., 2015. Impact of dataset diversity on accuracy and sensitivity
835 of parallel factor analysis model of dissolved organic matter fluorescence excitation-emission matrix. *Sci Rep* 5,
836 10207. <https://doi.org/10.1038/srep10207>
- 837 Zhang, H., Lauerwald, R., Regnier, P., Ciais, P., Van Oost, K., Naipal, V., Guenet, B., Yuan, W., 2022. Estimating the lateral
838 transfer of organic carbon through the European river network using a land surface model. *Earth Syst. Dynam.* 13,
839 1119–1144. <https://doi.org/10.5194/esd-13-1119-2022>
- 840 Zhuang, W.-E., Yang, L., 2018. Impacts of global changes on the biogeochemistry and environmental effects of dissolved
841 organic matter at the land-ocean interface: a review. *Environ Sci Pollut Res* 25, 4165–4173.
842 <https://doi.org/10.1007/s11356-017-1027-6>
- 843 Zhuang, W.-E., Chen, W., Cheng, Q., Yang, L., 2021. Assessing the priming effect of dissolved organic matter from typical
844 sources using fluorescence EEMs-PARAFAC. *Chemosphere* 264, 128600.
845 <https://doi.org/10.1016/j.chemosphere.2020.128600>
- 846 Zsolnay, A., Baigar, E., Jimenez, M., Steinweg, B., Saccomandi, F., 1999. Differentiating with fluorescence spectroscopy the
847 sources of dissolved organic matter in soils subjected to drying. *Chemosphere* 38, 45–50.